Dissertation

Regulation of sterol regulatory element binding protein (SREBP)-1c hepatic lipogenesis by adipose triglyceride lipase (ATGL)

Submitted by

Paola Patricia PEÑA DE LA SANCHA

For the Academic Degree of

Doctor of Philosophy (Ph.D.)

at the

Medical University of Graz

Diagnostic and Research Institute of Pathology

Under the Supervision of

Univ.-Prof. Dr. Gerald HOEFLER

2025

STATUTORY DECLARATION

I hereby confirm that the present diploma thesis is the result of my own independent scholarly work. I also confirm that in all cases, where material from the work of others (in books, articles, essays, dissertations, and on the internet) is acknowledged, quotations and paraphrases are clearly indicated. No material other than that cited in the reference list has been used. I have read and understood the Medical University's regulations and procedures concerning plagiarism. Furthermore, I hereby declare that if artificial intelligence (AI) tools were used for the generation and/or correction of certain text passages in the creation of this work, such employment was conducted in compliance with ethical principles, academic integrity, and the regulations of my university. Additionally, it was ensured that this usage was transparently disclosed and appropriately attributed."

Graz, May 5th 2025 Peña de la Sancha Paola Patricia.

DISCLOSURES

The present thesis is based on the following research article:

Peña de la Sancha, P., Wieser, B.I., Schauer, S. *et al.* Lipolysis-derived fatty acids are needed for homeostatic control of sterol element-binding protein-1c driven hepatic lipogenesis. *Commun Biol* 8, 588 (2025). https://doi.org/10.1038/s42003-025-08002-1

CO-AUTHOR CONTRIBUTIONS

- **Paola Patricia Pena de la Sancha (PPS):** designed, planned, and performed experiments; computed results; and wrote the manuscript.
- **Beatrix Irene Wieser (BIW):** designed, planned, and performed experiments; computed results; and wrote the manuscript.
- **Silvia Schauer (SS):** planned and performed experiments and computed results.
- **Helga Reicher (HR):** planned and performed experiments.
- **Wolfgang Sattler (WS):** planned and performed experiments.
- **Rolf Breinbauer (RB):** planned and performed experiments.
- **Martina Schweiger (MS):** planned and performed experiments.
- **Margarete Lechleitner (ML):** planned and performed experiments.
- **Saša Frank (SF):** planned and performed experiments.
- **Rudolf Zechner (RZ):** designed and planned experiments.
- **Dagmar Kratky (DK):** planned and performed experiments.
- **Peter John Espenshade (PJE):** planned and performed experiments.
- **Gerald Hoefler (GH):** designed and planned experiments and wrote the manuscript.
- **Paul Willibald Vesely (PWV):** designed, planned, and performed experiments; computed results; and wrote the manuscript.

PPS and **BIW** share first authorship as both contributed to the design, planning, and execution of the experiments in this work.
BIW performed experiments and evaluated the data from Figures 1 and 2.
PPS performed experiments and evaluated the data from Figures 1, 2, 3, 4, and 5.
PPS, BIW and PWV performed and analyzed experiments shown in Figure 6.
PPS, BIW, PV and GH analyzed data and wrote the manuscript.

The authorship order was assigned according to the number of experiments done for the manuscript.

ACKNOWLEDGMENTS

I thank the Austrian Science Fund (FWF) and the Metabolic and Cardiovascular Disease (DK-MCD) PhD Program [grant 10.55776/W1226] for funding this research.

I want to express my deep gratitude to Prof. Gerald Hoefler for allowing me to be part of his research group. It has been a privilege to learn from such a dedicated and experienced mentor, whose support and guidance were key for the completion of this work.

I acknowledge and deeply thank Dr. Paul W. Vesely for being my co-supervisor throughout my entire PhD. His constant guidance, input and contributions to the project made this work possible.

I thank Silvia Schauer for her continued support for this project, which greatly helped me to complete my PhD. I also thank my lab mates Manu Kanti and Huyen Phan, who made the stressful days more fun. I wish you all the best in your careers.

Many thanks to all the paper co-authors, their contribution and insights greatly enhanced the quality of this publication.

Thanks to my thesis committee members Dr. Dagmar Kratky, Dr. Ulrike Taschler, Dr. Robert Zimmermann and Dr. Guenter Haemmerle, for their continued support and advice, which greatly improved this project.

Thanks to the Medical University of Graz and the DK-MCD program for creating great opportunities for PhD students and allowing access to such a high-quality education. Special thanks to Karin Osibow for her commitment and always guiding students in our PhD journey.

I am deeply thankful to my parents Patricia de la Sancha Bahena and Jose Raul Peña de la Sancha, who have been beside me every step of the way, encouraging me to achieve my personal and professional goals. If today I have reached this milestone, it was because of your unconditional love and support since the day I was born. This achievement is also yours and I dedicate this work to you.

To my husband Mostafa Ezzat Ahmed, thank you for being my partner in life and throughout this journey. Your unconditional love and support made difficult times easier. Thanks for the sacrifices made, for your patience and permanent encouragement. This accomplishment also belongs to you.

TABLE OF CONTENTS

ABBREVIATIONS

Abbreviation	Definition
AAKO	ATGL knockout mice
ALKO	ATGL liver-specific knockout mice
AMPK	AMP-activated protein kinase
ATGL	Adipose Triglyceride Lipase
bHLHLZ	Basic Helix-Loop-Helix Leucine Zipper
DG	Diglyceride
ELISA	Enzyme-linked Immunosorbent Assay
ER	Endoplasmic Reticulum
FAs	Fatty Acids
GC/FID	Gas Chromatography/Flame Ionization Detection
GOLGI	Golgi Apparatus
HCD	High Carbohydrate Diet
HSL	Hormone Sensitive Lipase
INSIG	Insulin Induced Gene
LD	Lipid Droplets
LDL	Low Density Lipoprotein
LXR	Liver X Receptor
MM	Membrane Extracts
MGL	Monoglyceride Lipase
mTOR	Mammalian Target of Rapamycin complex
NAFLD	Non-Alcoholic Fatty Liver Disease
NEFAs	Non-Esterified-Fatty Acids
NEX	Nuclear Extracts
NLSD	Neutral Lipid Storage Disease
PI3K	Phosphoinositide 3-kinases
PPAR	Peroxisome proliferator-activated receptor
PUFA	Polyunsaturated Fatty Acids
sNEFAs	Saturated Non-Esterified Fatty Acids
SCAP	SREBP Cleavage-Activating Protein
sFAs	Saturated Fatty Acids
SREBP	Sterol Regulatory Element Binding Proteins
SREBP-1c	Sterol Regulatory Element Binding Protein-isoform 1c
TGs	Triglycerides
UBXD8	UBX Domain-Containing protein 8
uFAs	Unsaturated Fatty acids
uNEFAs	Unsaturated Non-Esterified Fatty Acids

ZUSAMMENFASSUNG

Sterol Regulatory Element-Binding Proteins (SREBP) sind eine Gruppe von Transkriptionsfaktoren, die in der Membran des Endoplasmatischen Retikulums (ER) synthetisiert werden und die Lipogenese regulieren. Unter den SREBP-Isoformen (SREBP-1a, -1c und -2) aktiviert SREBP-1c bevorzugt die Transkription von Genen, die für die Synthese von Fettsäuren (FS) und Triglyceriden (TG) erforderlich sind. Im Gegensatz dazu wird beim Fasten die Lipogenese unterdrückt und die Hydrolyse der im Fettgewebe gespeicherten TGs aktiviert. Dadurch werden Glycerin und FS freigesetzt, die in verschiedene Gewebe transportiert werden, um Energie zu liefern (Lipolyse). Die Adipose Triglyceride Lipase (ATGL) ist das Enzym, das den ersten und limitierenden Schritt der Lipolyse in Lipidtröpfchen (LD) katalysiert. Darüber hinaus hat ATGL eine Affinität zur Hydrolyse ungesättigter Fettsäuren (uFAs), die proteolytische Aktivierung von SREBP-1c in vitro regulieren. Daher gehen wir davon aus, dass die aus der ATGL-Lipolyse gewonnenen FAs die SREBP-1c-Regulation in der Leber beeinflussen können, indem sie die proteolytische Aktivierung von SREBP-1c während des Fastens hemmen. Um unsere Hypothese zu testen, analysierten wir die hepatische SREBP-1c-Regulation in fettspezifischen ATGL-Knockout-Mäusen (AAKO) oder leberspezifischen ATGL-Knockout-Mäusen (ALKO).

Unsere Ergebnisse zeigten, dass Mäuse mit selektiver ATGL-Deletion im Fettgewebe oder in der Leber nach Fasten und darauf folgender Aufnahme einer kohlenhydratreichen Diät (HCD) eine vorübergehende Hochregulierung von SREBP-1c in der Leber aufwiesen. Darüber hinaus wiesen AAKO-Mäuse während des Fastens signifikant weniger ungesättigte, nicht veresterte Fettsäuren (uNEFAs) im Plasma und in der Leber auf. Weiters entwickelten wir einen adenoviralen Flag-SREBP-1c-Spaltungsreportervektor, der zeigte, dass die hepatische SREBP-1c-Aktivierung in AAKO-Mäusen während des Fastens verstärkt ist. Interessanterweise kehrte die exogene Zufuhr von albumingebundenen uFAs während des Fastens diesen Effekt um. Zur Unterstützung dieser Ergebnisse zeigten mit dem Flag-SREBP-1c-Reporter transfizierte HepG2-Zellen, dass die Behandlung mit uFAs die hepatische SREBP-1c-Aktivierung signifikant herunterregulierte. Im Gegensatz dazu zeigte die Behandlung mit gesättigten Fettsäuren (sFA) keinen Effekt. Schließlich wurde in mit uFAs behandelten primären Hepatozyten der Transport des SREBP-Spaltungsaktivierungsproteins (SCAP) vom ER zum Golgi-Apparat gehemmt, was einen kritischer Schritt bei der proteolytischen Aktivierung von SREBP darstellt.

Die Ergebnisse unserer *In vitro* und *In vivo* Modelle legen nahe, dass während des Fastens die ATGL-vermittelte Lipolyse Fettsäuren aus dem Fettgewebe in den Kreislauf freisetzt, die dann zur Leber transportiert werden, wo sie die SREBP-1c-Aktivierung regulieren. Diese Ergebnisse weisen auf eine neuartige ATGL/SREBP-1c-Crosstalk-Regulation der hepatischen Lipogenese hin.

ABSTRACT

Sterol Regulatory Element-Binding Proteins (SREBPs) are a group of transcription factors synthesized in the Endoplasmic Reticulum (ER) membrane that regulate cellular lipogenesis. Among the SREBP isoforms (SREBP-1a, -1c, and -2), SREBP-1c preferentially activates the transcription of genes required for the synthesis of fatty acids (FAs) and triglycerides (TGs). Conversely, during fasting, lipogenesis is suppressed, and the hydrolysis of TGs stored in the adipose tissue is activated, releasing glycerol and FAs that are transported to different tissues to provide energy in a process known as lipolysis. Adipose Triglyceride Lipase (ATGL) is the enzyme that catalyzes the first and limiting step in lipolysis within lipid droplets (LDs). In addition, ATGL has an affinity for the hydrolysis of unsaturated fatty acids (uFAs), which have been shown to regulate the proteolytic activation of SREBP-1c *in vitro*. Therefore, we propose that the FAs derived from ATGL lipolysis can influence SREBP-1c regulation in the liver by inhibiting the proteolytic activation of SREBP-1c during fasting. To test our hypothesis, we analyzed the hepatic SREBP-1c regulation in Adipocyte-specific ATGL knockout (AAKO) or ATGL liver-specific knockout mice (ALKO).

Our results demonstrated that mice with selective ATGL deletion in adipose tissue or liver exhibited transient hepatic SREBP-1c upregulation after fasting and refeeding a high carbohydrate diet (HCD). Additionally, AAKO mice showed significantly lower plasma and liver unsaturated non-esterified fatty acids (uNEFAs) during fasting. Furthermore, we developed an adenoviral Flag-SREBP-1c cleavage-reporter vector, which evidenced that hepatic SREBP-1c activation is enhanced in AAKO mice during fasting. Interestingly, the exogenous supply of albumin-bound uFAs during fasting reversed this effect. In support of these findings, HepG2 cells transfected with the Flag-SREBP-1c reporter showed that treatment with uFAs significantly downregulated hepatic SREBP-1c activation. In contrast, treatment with saturated FA (sFA) had no effect. Finally, in primary hepatocytes treated with uFAs, the transport of the SREBP Cleavage-Activating Protein (SCAP) from the ER to the Golgi Apparatus was inhibited, which is a critical step in SREBP proteolytic activation.

The results from our *in vitro* and *in vivo* models suggest that during fasting, ATGL-mediated lipolysis releases FAs from adipose tissue into the circulation, that are then transported to the liver, where they regulate SREBP-1c activation. These findings evidence a novel ATGL/SREBP-1c crosstalk regulation for hepatic lipogenesis.

1. INTRODUCTION

Energetic balance plays a crucial role in maintaining metabolic homeostasis. The equilibrium between the expenditure and storage of energy obtained from the diet, requires a constant and dynamic fluctuation between catabolic and anabolic pathways, orchestrated by a complex hormonal, enzymatic, and transcriptional interaction that contributes to cellular homeostasis.

In circumstances where dietary intake surpasses metabolic needs, the excess energy is transformed into fatty acids (FAs), which are subsequently esterified and stored as triglycerides (TGs) in the adipose tissue, in a process known as lipogenesis. Sterol Regulatory Element-Binding Proteins (SREBPs) are the master transcriptional regulators of cellular lipid synthesis and are responsible for the transcription of genes involved in lipogenesis (1-4).

Conversely, in situations where the energetic demand increases, such as fasting or during exercise, lipogenesis is downregulated, and energy is obtained through lipolysis. Adipose Triglyceride Lipase (ATGL); the main regulatory enzyme for lipolysis, supplies the organism with FAs released from the TG stored in the adipose tissue for energy production (1).

The FAs produced by ATGL lipolysis act as signaling molecules that activate other metabolic pathways or work as ligands to activate transcription factors. ATGL possesses an affinity for the hydrolysis of unsaturated fatty acids (uFAs) (5). At the same time, uFAs have been shown to regulate Sterol Regulatory Element-Binding Protein-1c (SREBP-1c), the primary SREBP isoform involved in FA biosynthesis. Hence, we propose that the uFAs released by ATGL from the adipose tissue can regulate SREBP-1c lipolysis in the liver (6).

The disturbances in the equilibrium between lipogenesis and lipolysis, are related to the development of metabolic disorders, such as insulin resistance and dyslipidemias, that underlie the development of diseases like nonalcoholic fatty liver disease (NAFLD),

atherosclerosis, diabetes and obesity, which constitute the leading causes of death worldwide and represent a burden for the health of individuals and the health care systems around the world (7) (8). Therefore, in this study we explored the interaction between lipogenesis and lipolysis and propose that these metabolic pathways converge through an SREBP-1c / ATGL interaction, bringing new insights for the understanding of the molecular mechanisms that lead to the development of these metabolic disturbances.

1.1 Sterol Regulatory Element Binding Proteins

Lipids are a diverse group of organic molecules involved in a wide range of fundamental biological functions. They are structural components of cell membranes, precursors of hormones, act as signaling molecules and constitute the main energy source in the organism. Lipids can be obtained exogenously through dietary intake or synthesized endogenously by lipogenesis. Lipid synthesis occurs in every cell, but the liver and white adipose tissue play a central role in the synthesis and storage of lipids (1-4).

Nevertheless, the excessive accumulation of lipids is toxic to cells, causing a harmful environment known as “lipotoxicity”, which is related to metabolic disturbances that underlie the development of cardiovascular and metabolic diseases. Therefore, lipogenesis is a highly regulated process at the transcriptional and post-transcriptional level to maintain energetic and cellular homeostasis. Sterol Regulatory Element Binding Proteins (SREBPs) are a group of transcription factors that constitute the central regulators of lipogenesis in the cell (9, 10).

SREBPs were first described by the Goldstein and Brown group (11), who defined a group of proteins that regulate cellular cholesterol and FA biosynthesis. Since then, growing evidence showed that SREBP disturbances are implicated in metabolic and cellular abnormalities, like mitochondrial dysfunction, abnormal cell proliferation, inflammation, autophagy, oxidative stress and ER stress, which play a significant role in the development of dyslipidemia, diabetes, obesity, NAFLD and cancer, among other pathologies (9, 12).

SREBP’s are synthesized as 1150 amino acid length inactive precursor proteins in the ER membrane. They belong to the basic helix-loop-helix leucine zipper (bHLHLZ) transcription factor family. Their structure is constituted by an NH-2 transmembrane domain, which contains a transactivation domain, and a COOH-terminal regulatory domain, both oriented to the cytosol and linked by a 30 amino acid loop in a hairpin domain projected into the ER lumen (2, 12-14), as depicted in the Introductory Figure 1.

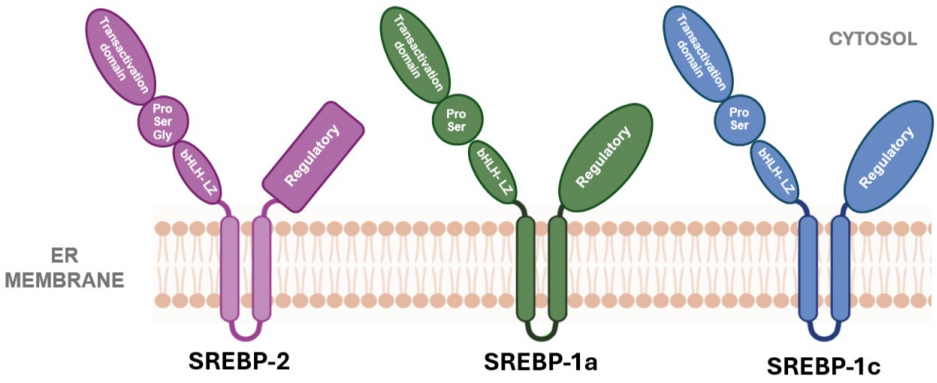

Introductory Figure 1. Sterol Regulatory Element Binding Proteins (SREBPs) structures. SREBPs are conformed by three different isoforms: SREBP-2, SREBP-1a and SREBP-1c. Their structure includes an N-terminal domain facing the cytosol that contains the transactivation domain, a proline and serine-rich region, and the basic helix-loop-helix leucine zipper (bHLH-LZ) region. Next, two transmembrane segments connected by a short amino acid loop that faces the ER lumen and the C-terminal segment that contains the SREBP regulatory domain. *Modified from Eberle et al. 2004. (2)*

The SREBP family is constituted by three isoforms; SREBP-1a, SREBP-1c and SREBP-2, that are encoded by two different genes. Together, they regulate the synthesis of cholesterol and FAs in the cell, but they are regulated differently. SREBP-2 is encoded by the SREBF2 gene and regulates the transcription of genes and enzymes involved in cholesterol synthesis by a strict feedback regulation. The genes transcribed by SREBP-2 include LDL-receptor (LDL-R), 3-hydroxy-3-methyl-glutaryl-coenzyme A reductase (HMGCR) and HMG-CoA synthase (HMGCS) (15).

The SREBP-1 family consists of SREBP-1a and SREBP-1c isoforms. Both are transcribed from the same gene (SREBF1), but their structures differ in the first exon (exon-1a and -1c) (Introductory Figure 1). As a result, they are activated by different promoters through alternative splicing. SREBP-1a is mainly expressed in immortal cell lines, whereas SREBP-1c is the predominant form in most tissues, especially in the liver and white adipose tissue. SREBP-1a is involved in both cholesterol and FA synthesis, while SREBP-1c preferentially activates the transcription of genes for FA and TG synthesis like *Srebf1, Acaca, Fasn* and *Scd1* (12, 16, 17).

SREBPs need to be proteolytically processed in order to be activated. However, the cleavage-activation of each SREBP isoform is regulated by different stimuli, as described below.

1.2 SREBP cleavage activation

SREBPs are synthesized as precursors in the ER membrane and require interaction with other proteins to be transported to the Golgi apparatus, where they undergo proteolytical cleavage to activate the transcription of lipogenic genes in the cell nucleus (18). In the ER membrane, SREBPs form complexes with INSIG (Insulin-Induced Gene Proteins), which include INSIG-1 and INSIG-2 isoforms, and with SCAP (SREBP Cleavage-Activating Protein), which together regulate their transport and cleavage activation (9, 15, 19-21).

After SREBPs are transcribed in the ER membrane as inactive precursors (P-SREBP), SCAP binds to the C-terminal domain of SREBP, creating the SREBP-SCAP complex. When FA or sterol levels are adequate in the cell, oxysterols bind to INSIG and stabilize it, retaining the SREBP-SCAP complex in the ER, preventing its transport to the Golgi apparatus and, in consequence, inhibiting the transcription of the genes involved in lipogenesis (22-25).

In contrast, when uFAs or sterol levels decrease, INSIG is translocated to the cytosol, where it is ubiquitinated by E3 ligases and then degraded. Consequently, SCAP binds to COPII vesicles, which include Sec23 and Sec24 proteins, that allow the transport of the SREBP-SCAP complex to the Golgi apparatus, where SREBP is proteolytically processed by S1P (Site-1-Protease) and S2P (Site-2-Protease) proteases that cleave SREBP in two steps (17, 19, 23).

First, S1P cleaves the SREBP protein in half, and next, S2P cleaves the transcriptionally active N-terminal domain (N-SREBP) that is transported to the cell nucleus, where it activates the transcription of the genes involved in cholesterol and FA synthesis, as depicted in the Introductory Figure 2. Importantly, SREBP cleavage-activation processing is controlled by multiple transcriptional factors that modulate SREBPs mediated lipogenesis (2, 9, 15, 17).

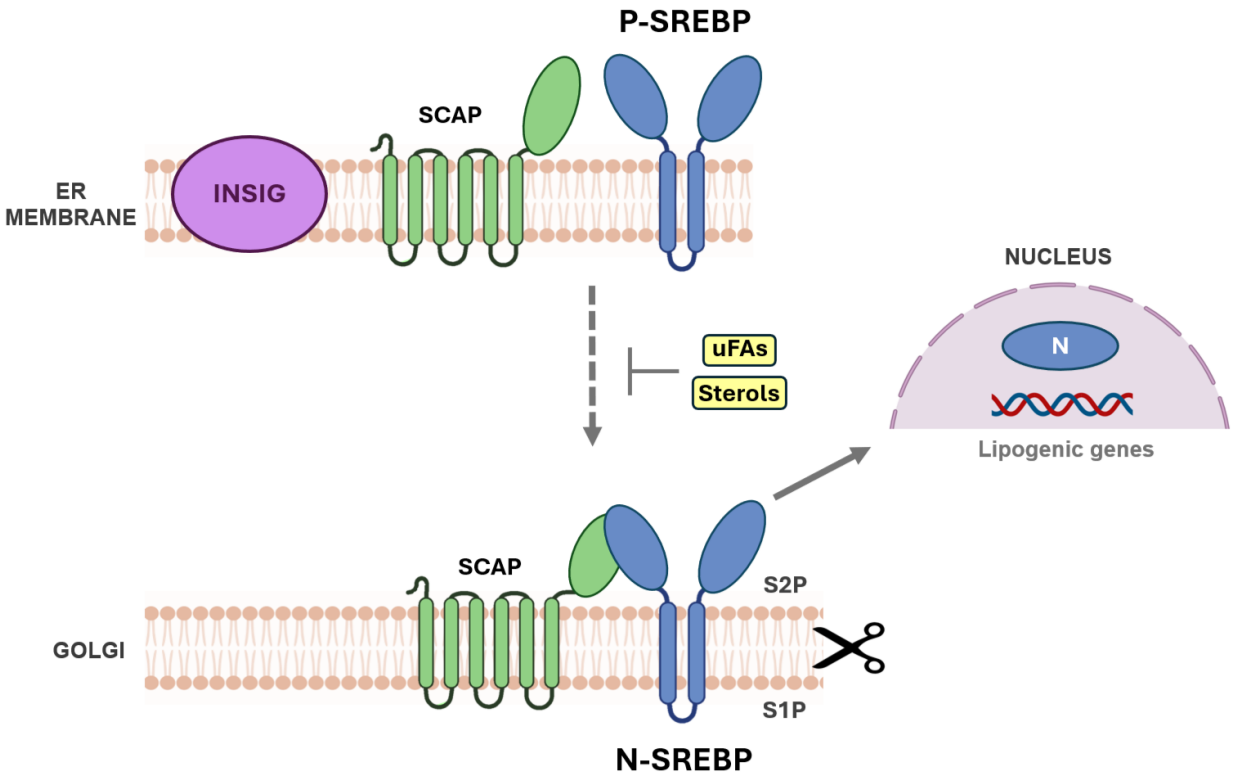

Introductory Figure 2. SREBP cleavage regulation. SREBPs are synthesized in the Endoplasmic Reticulum (ER) membrane as precursor proteins (P-SREBP), where they form complexes with other proteins, such as INSIG (Insulin-Induced Gene Proteins) and SCAP (SREBP Cleavage-Activating Protein). When lipids in the cell are low, the SREBP-SCAP complex is transported to the Golgi apparatus, where the nuclear SREBP (N-SREBP) is processed by S1P and S2P proteases, releasing the N-Terminal domain that, in the nucleus of the cell, activates the transcription of genes involved in lipogenesis. *Adapted from Shimano et al., 2017 (9)*

1.3 Transcriptional regulation of SREBP-1c

SREBP activation is modulated at multiple levels. However, their transcriptional regulation is key for SREBP mediated lipogenesis, and it is controlled by three main factors: first, the Sterol Regulatory Element (SRE) in the promoter region of SREBP target genes. The second is the stimulation of SREBP-1c transcription by insulin, and the third is Liver X-activated Receptors (LXRs) -induced SREBP-1c expression. However, SREBP-1 and SREBP-2 exhibit significant differences in their transcriptional regulation and are activated by different stimuli (22, 26, 27).

SREBP-2 transcription and proteolytic processing are mainly regulated by sterols from endogenous synthesis, such as oxysterols and 25-hidroxycholesterol (25-HC). The structure of SREBP-2 contains a sterol-sensitive domain that binds to the SRE sequence of the genes involved in the cholesterol synthesis pathway (9).

On the other hand, SREBP-1c activation is mainly regulated by FA in the liver and, unlike SREBP-1a and SREBP-2 isoforms, it is highly sensitive to nutritional status. Therefore, its regulation is especially important for hepatic lipogenesis (9, 19). In nutrient-abundant states, such as postprandium, hepatic lipogenesis is induced to metabolize the excessive intake of energy to be used as substrate for other energetic pathways or transformed into FAs that are esterified and later stored as TG in the LDs of the adipose tissue, in a process induced by hepatic SREBP-1c activity. As a result, the activation of SREBP-1c is regulated by the fasting and feeding cycle (9, 28, 29).

These observations emerged after Horton *et al*., observed that P-SREBP-1c transcription was very low in mice that were fasted overnight. Conversely, when mice were fed a low fat / high carbohydrate diet (HCD) after prolonged fasting, N-SREBP-1c activation was strongly induced in the liver, as well as the transcription of genes involved in FA synthesis (30, 31).

This is explained by the fact that SREBP-1c is highly regulated by glucose and insulin, the main anabolic hormone in the body, which acts as a key regulator for FA synthesis in the liver by inducing SREBP-1c transcription. During fasting, insulin levels are low,

and cAMP is induced by the action of glucagon, inhibiting SREBP-1c transcription. Conversely, after feeding a HCD, blood glucose levels rise and induce the secretion of insulin, promoting SREBP-1c transcription (17, 28, 32). Insulin also promotes the transcription of INSIG-1 protein, while INSIG-2 is suppressed during feeding and upregulated during fasting, which together modulate SREBP-1c cleavage activation (31, 33, 34).

Insulin regulates lipid metabolism and SREBP-1c transcription through the action of diverse kinases that belong to the PI3K–AKT–mTOR pathway. AKT induces hepatic lipogenesis through SREBP-1c. At the same time, mTORC (mammalian target of rapamycin complex) activates AKT by phosphorylating it at the serine-473 residue. Additionally, hepatic p-S6 kinase is a key regulator of mTORC that also regulates SREBP. During fasting, AMPK inhibits the mTORC pathway, and SREBP-1c-mediated lipogenesis is suppressed (2, 19, 35, 36).

Importantly, SREBP-1c response to insulin is also mediated through LXRs, which are nuclear transcription factors involved in lipid metabolism that induce SREBP-1c transcription and consist of two isotypes, LXR-α and LXR-β (2) (37). LXRs bind to the LXR response element (LXRE) of a wide range of genes involved in hepatic FA biosynthesis like *Srebf1c, Fasn* and *Scd1* genes, which raise plasma TG levels (38-40).

1.4 SREBP-1c regulation by unsaturated fatty acids

Several groups have demonstrated that FAs, mainly of the unsaturated species, play an important role in SREBP-1c regulation through different mechanisms. *In vitro* studies have shown that uFAs regulate the SREBP-SCAP complex transport to the Golgi by controlling the stability of INSIG-1, which plays a central role in the feedback regulation of SREBP processing. In contrast, treatment with saturated fatty acids showed no effect (21).

In studies using HEK-2 cells, uFAs blocked SREBP-1 proteolytic processing and decreased its target gene expression, while SREBP-2 was not affected (41). Additionally, HepG2 cells treated with Arachidonic acid (AA) and Eicosapentaenoic acid (EPA) decreased *Srebf1* expression up to 90%, as well as a significant decrease in SREBP-1c protein (23).

Therefore, the inhibitory effect of uFAs on SREBP-1c transcription and proteolytic processing is proposed to be achieved by different mechanisms. First, uFAs inhibit SREBP-1c proteolytic processing by competitive inhibition of LXRs**,** which promote SREBP activation (22) (26). Additionally, uFAs have shown to increase SREBP-1c mRNA degradation (28) (42).

Furthermore, uFAs block the proteolytic processing of SREBP-1 by a mechanism that involves Ubiquitin regulatory X domain-containing protein 8 (UBXD8), which is a protein that interacts with the polyubiquitin chains (Ub) attached to INSIG-1 through GP78. UFAs form a complex with UBXD8, inhibiting binding between UBXD8 and INSIG1, which stabilizes INSIG and prevents its degradation. The increased levels of INSIG-1, retain the SREBP1–SCAP complex in the ER, inhibiting SREBP1 target genes.

When uFAs are scarce, INSIG levels decline, and as a result, SREBP-SCAP complex lose their ER-anchors, allowing FA synthesis by N-SREBP-1c. To avoid the toxic effect of NEFAs, the FA produced by SREBP-1c lipogenesis are stored as TG in the lipid droplets in the adipose tissue (10) (6) (43) (44) (45) (41).

On the other hand, *de novo* lipogenesis is not the only source of FAs. When energetic demands increase and metabolism is under energy deficit, the TGs stored in the adipose tissue lipid droplets are degraded to obtain FAs that are used as energy substrates to reestablish the energy balance (9).

1.5 Lipolysis regulation

When the energy intake exceeds the metabolic needs, the excess FAs are esterified and stored as TG in lipid droplets (LD), which are cellular organelles involved in fat storage and lipid metabolism (46). Most cells contain LD for neutral lipid storage to avoid the harmful effects of non-esterified fatty acids (NEFAs) in cells, or to be used as a reserve of energy. The white adipose tissue (WAT) represents the biggest energy source and reservoir in the body (47) (48) (49) (50) (51).

In situations where the energy demand increases, such as fasting or during exercise, NEFAs must be released from adipose tissue TG to the plasma to supply organs and tissues with energy by a process known as lipolysis (47). Lipolysis consists of the enzymatic degradation of TG stored in cellular LD to generate FA and glycerol, and it is regulated by the sequential action of three lipases (48) (49).

Initially, Hormone Sensitive Lipase (HSL), was believed to be the rate-limiting enzyme of lipolysis. However, Zimmermann et al., (52) and two other groups, discovered simultaneously that an additional lipase could still hydrolyze the TG, releasing FA even in the absence of HSL. This enzyme was named adipose triglyceride lipase (ATGL) which is the main regulatory enzyme for lipolysis, and it catalyzes the initial step of TG hydrolysis, generating diglycerides (DGs) and FA (47-49, 52). Next, the resulting DGs are hydrolyzed by HSL, generating monoglycerides (MG) and FA. Finally, Monoglyceride Lipase (MGL) cleaves the last FA off the MG, releasing FA and glycerol, as depicted in Introductory Figure 3.

Lipolysis raises plasma NEFA concentration and increases the FA uptake by the liver (47, 53) (54). ATGL hydrolyzes TGs preferentially at the sn-2 position of the glycerol

backbone. Interestingly, it has been shown that ATGL possesses an affinity for uFA hydrolysis (51, 52, 55).

The FAs released from lipolysis perform various metabolic roles; they can function as energy substrates for ATP production through β-oxidation, serve as structural elements of the cellular membrane, and act as ligands to activate the transcription of other factors and gene expression (47) (56).

Importantly, lipolysis generates ligands for the activation of a group of transcription factors called Peroxisome Proliferator-Activated Receptors (PPARs) that are involved in a broad range of metabolic functions. The FAs generated during lipolysis have been shown to act as PPAR ligands (5).

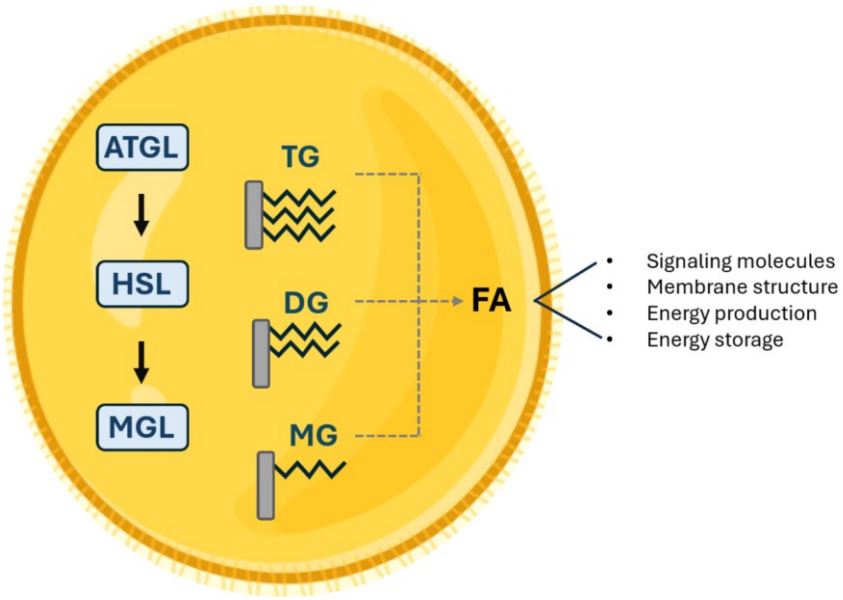

Introductory Figure 3. Lipolysis in the lipid droplet. During fasting, fatty acids (FAs) are supplied by the hydrolysis of triglycerides (TG) from adipose tissue lipid droplets by the sequential action of three lipases. In the first step, TGs are hydrolyzed by Adipose Triglyceride Lipase (ATGL), generating diglycerides (DGs) and FAs. These DGs are then hydrolyzed by Hormone Sensitive Lipase (HSL), generating monoglycerides (MG) and FAs. In the final step, Monoglyceride Lipase (MGL) cleaves the last FA off the MG, releasing glycerol and FAs. The FAs released during lipolysis fulfill diverse metabolic and physiological functions; they can be incorporated into other metabolic pathways for energy storage or production or act as signaling molecules involved in other cellular processes. *Adapted from Schreiber R. et al.* (1)

1.6 ATGL regulation

The gene encoding ATGL in humans is the Patatin-like phospholipase domain containing 2 *(PNPLA2*), also known as *Atgl* (1). The catalytic site of ATGL is located within the patatin domain at the N-terminus domain and the C-terminal portion contains a hydrophobic lipid droplet-binding region. ATGL is present in most tissues, but is mainly expressed and active in white and brown adipose tissue (49) (52, 57).

ATGL activity is induced by the action of its co-activator protein CGI-58 (Comparative gene identification-58) also known as ABHD5, that directly binds to ATGL and induces its activity. Additionally, ATGL transcriptional regulation is mediated by peroxisome proliferator-activated receptor gamma (PPAR-γ) and inhibited by G0S2 protein (G0/G1 switch protein 2) (1) (57).

ATGL function is affected by nutritional status, and its function is dependent on different hormones; catecholamines induce ATGL through the activation of β-adrenergic receptors. In contrast, insulin is a potent inhibitor of lipolysis. Therefore, ATGL mRNA is induced during fasting and suppressed during feeding states (1, 52) (58).

To further elucidate the metabolic impact of *Atgl* genetic deletion, various ATGL-knockout (KO) animal models lacking *Atgl* systemically or in specific tissues have been established (1).

1.7 Metabolic effects of ATGL deletion in mice

In humans, mutations in the PNPLA2 gene produce neutral lipid storage disease (NLSD), which is characterized by an accumulation of lipids in different tissues, mainly the heart, producing cardiomyopathy that leads to premature death (48) (10) (59). In mice, ATGL-KO animals exhibit impaired lipolytic activity that leads to an accumulation of lipid deposits in most organs. Systemic ATGL-KO mice present defective lipolysis, cold intolerance and dramatic accumulation of TG in the cardiac muscle that leads to cardiomyopathy and premature death as a consequence of heart dysfunction (10, 60, 61).

Liver-specific ATGL knockout mice (ALKO) show marked hepatic steatosis characterized by a 3-fold higher TG content in the liver compared to control mice. However, they show normal insulin levels, glucose tolerance, and cold and fasting tolerance (62).

On the other hand, the absence of ATGL in adipose tissue results in a suppressed release of FA from adipose-LDs. Consequently, Adipocyte-specific ATGL knockout (AAKO) mice show a significant reduction in plasma NEFA concentration during fasting compared to controls. However, they show improved insulin sensitivity and glucose tolerance compared to control mice. Additionally, these mice exhibit cold intolerance due to the lack of FA to fuel thermogenesis (50, 57, 60, 63). In AAKO mice, carbohydrates become the main energy substrates apparently as an adaptive response to compensate for the FA deficit (1) (61).

1.8 Importance of studying SREBP-1c / ATGL regulation.

Hepatic lipogenesis is regulated by SREBP-1c, the master transcription factor for FA synthesis. On the other hand, ATGL releases FAs from adipose tissue stores in situations of high energy demand through lipolysis that are transported to the liver for energy synthesis. Therefore, SREBP-1c and ATGL are critical for lipid and energy homeostasis in the organism.

Interestingly, FAs act as metabolic intermediaries that regulate other signaling pathways in both lipogenesis and lipolysis. Importantly, ATGL preferentially hydrolyzes uFA species from TG in the LDs. For instance, adipose ATGL-KO mice display significantly decreased plasma NEFA concentration during fasting and uFAs are especially reduced (55, 60). Interestingly, *in vitro* studies demonstrated that the same FA species modulate SREBP-1c through their proteolytic regulation in the ER membrane (6, 26, 41, 44, 45). Additionally, Schreiber *et al*., found that SREBP-1c was significantly reduced in Adipocyte-specific ATGL-KO mice, which indicates a possible role of ATGL in SREBP-1c activation (64).

However, up to date, no studies have demonstrated whether FA derived from ATGL lipolysis can modulate SREBP-1c activation in the liver and the role of FA on hepatic SREBP-1c regulation *in vivo*. Therefore, understanding the relationship between lipolysis and lipogenesis through a potential ATGL/SREBP-1c interplay can help us understand the molecular mechanisms that underlie the development of metabolic and cardiovascular diseases.

Hence, we propose that the FAs derived from ATGL lipolysis can regulate hepatic SREBP-1c lipogenesis. To understand the role of ATGL-derived FAs in the regulation of SREBP-1c hepatic lipogenesis, we used Adipocyte-specific ATGL knockout (AAKO) (61) and Liver-Specific ATGL-KO mice (ALKO) (62).

2. MATERIALS AND METHODS

Peña de la Sancha et al., (65) previously published the methods contained in this section as an original article in Nature Communications Biology. Therefore, the text in the following materials and methods section has been partially or fully adapted from the mentioned article.

Animals

The animals were obtained from our own breeding. Animals were kept in a pathogen-free environment, on a dark/light cycle of 14 h light /10 h dark, at 22 ± 1°C.

Under non-experimental conditions, the animals were fed a standard chow diet (4.5% fat, 34% starch, 5.0% sugar and 22.0% protein) M-Z extrudate, V1126, Ssniff Spezialdiäten, Germany

Mouse strains used:

- **AAKO:** Adipose-tissue specific *Atgl*-knockout (*Atgl*$^{flox/flox}$, *Adipoq-Cre*) C57Bl/6J background (61);
- **ALKO:** Liver-specific *Atgl*-knockout (*Atgl*$^{flox/flox}$, *Alb-Cre*) C57Bl/6J background (62).
- **Wild Type:** C57Bl/6J (own breeding, originally from Jackson lab).

Fasting/refeeding experiments

Mice were either fasted for 12 h overnight (fasted group) or fasted and then refed with a special diet (Refed group). For the fasted group, the food was removed from 6 p.m. to 6 a.m and then the mice were sacrificed. The refed group was fasted overnight and then refed a high carbohydrate/low-fat diet (HCD, TD 88122; Harlan Teklad, USA), and then sacrificed after 3 h, 6 h or 9 h after HCD refeeding.

Experiments using special diets

- Saturated FA-rich diet: Mice were fed ad libitum for 3 consecutive days with a saturated FA diet (100 g of chow powder food, 50 g of casein and 60 mL of palm oil) and subsequently sacrificed.
- Unsaturated FA-rich diet: Mice were fed ad libitum for 3 consecutive days with an unsaturated FA diet (100 g of chow powder food, 50 g of casein and 60 mL of flaxseed oil) and subsequently sacrificed.

Albumin-bound FA infusion

Mice were fasted for 12 h from 7 p.m. to 7 a.m. or fasted and intravenously injected with bovine serum albumin complexed oleic acid (18:1, BSA-Oleate Monounsaturated FA Complex (5 mM) Item No. 29557, Cayman Chemical) 3 and 9 h after food withdrawal. Mice were sacrificed 3 h after the second FA infusion.

Liver microsomal and nuclear fractionations

The protocol from Engelking, L.J *et al*. was followed with minor modifications (66). On the day of sacrifice, mouse livers were harvested and washed twice in ice-cold PBS, then frozen in methylbutane cooled with liquid nitrogen.

- **Nuclear fraction isolation (NEX)**

600 mg of frozen liver were mixed with 6 ml buffer A (10 mM Hepes at pH 7.6, 25 mM KCl, 1 mM sodium EDTA, 2 M sucrose, 10% vol/vol glycerol, 0.15 mM spermine, 2 mM spermidine, 1x protease Inhibitor cocktail, 50 µg/ml ALLN). Livers were homogenized with a Teflon pestle in a potter homogenizer at low speed. The homogenate was filtered through a 100 µM cell strainer. Samples were overlaid with 2 ml buffer A in SW 41Ti tubes, and the tubes filled with Buffer 1 (10 mM Hepes at pH 7.6, 25 mM KCl, 1 mM sodium EDTA). The samples were then centrifuged at 25,000 rpm (75,000 g) for 1 h at 4°C in a SW 41 Ti Rotor. Subsequently, the tubes were turned over (the supernatant was collected for later use to isolate microsomal membrane extracts) and nuclear pellet was recovered from the bottom and resuspended in 1 ml buffer D (10 mM Hepes pH

7.6, 100 mM KCl, 2 mM $MgCl_2$, 1 mM sodium EDTA, 10% (vol/vol) glycerol, 1 mM DTT, 1x protease inhibitor cocktail, 50 µg/ml ALLN). For extraction of soluble nuclear proteins, we added 140 µl of buffer AS (3.3 M ammonium sulfate (pH 7.9), then agitated for 40 min at 4°C on a rotating wheel in a cold room. Then the sample was centrifuged at 78,000 rpm in Beckman TLA-100.4 rotor for 45 min at 4°C. The supernatant was mixed 1:5 with 5x FSB and designated soluble nuclear protein extract (NEX).

- **Microsomal membrane extracts isolation (MM)**

For membrane fractions isolation, 1 mL from the supernatant previously collected after the first centrifugation cycle was resuspended in 9 mL buffer M (20 mM Tris-HCl pH 7.4, 2 mM $MgCl_2$, 0.25 mM sucrose, 10 mM sodium EDTA, 10 mM sodium EGTA, 1x protease inhibitor cocktail, 50 µg/ml ALLN). The homogenate was centrifuged at 30,000 rpm for 1 h at 4°C in a SW41 Ti Rotor. The resulting pellet was dissolved in 1x FSB and designated cytosolic microsomal membrane extract (MM).

Cell culture media and supplements

Mevastatin (M2537), mevalonate (50838) and *N*-acetyl-leucinyl-leucinyl-norleucinal (ALLN, 208719) were obtained from Merck, Germany; 25-hydroxycholesterol (25-HC, H1015), lipoprotein-deficient serum (LPDS; S5394), ITS Liquid Media Supplement (100×) (ITS, I3146), Forskolin (F3917) were purchased from Sigma Aldrich.

Fetal bovine serum (FBS, 10500), high glucose Dulbecco's modified Eagle's medium (DMEM, 41966052) and penicillin-streptomycin (PenStrep, 15140-122) were obtained from Gibco, USA. There reagents were used to prepare the following culture mediums:

- Cell culture medium: DMEM containing 1x PenStrep and 10% (v/v) FBS.
- Hepatocyte medium: DMEM containing 1x PenStrep, 20% (v/v) FBS, 100 nM dexamethasone, 1x ITS-Supplement.
- 5% LPDS medium: DMEM containing 1x PenStrep and supplemented with 5% (v/v) LPDS (Sigma Aldrich, USA, S5394).

BSA bound FAs

Different FAs were bound to BSA; 4 mM FA sodium salt (sodium palmitate (Cayman, P9767); palmitoleic acid sodium salt (Sigma Aldrich, USA, 6610-24-8); sodium oleate (Sigma Aldrich, USA, O75011); linoleic acid sodium salt (Sigma Aldrich, USA, L8134) solutions in double distilled H_2O, and mixed with 172 mg/ml (w/v) FA free BSA (Sigma Aldrich, USA, A7030) in 2x PBS at 37° under constant vortexing.

HepG2 cell line experiments

HepG2 cells were cultured under standard cell culture conditions at 37°C, 5% CO_2 in D10F medium. For experiments, cells were seeded at 70% confluence in 6-well plates. After one day, HepG2 cells were transfected using Lipofectamine 3000 (Thermo Fisher, L30000-08, Germany) with 1.6 µg of Flag-SREBP-1c vector containing human *SREBF1* cDNA. 48 hours later, the cells were washed with PBS and incubated in 5% LPDS, or 5% LPDS plus the addition of 100 µM BSA bound FA or, 2.5 µM 25-HC for 16 h. Two hours before harvest, 25 µg/ml ALLN was added. Cells were harvested directly in FSB (final sample buffer: 60 mM Tris-HCl at pH 7,4; 2% (w/v) SDS; 10% glycerol) and analyzed by WB.

Construction of an *in vivo* SREBP-1c cleavage-reporter vector

The *SREBP-1c* cDNA was isolated by enzymatic restriction from the pQCXIN vector (Addgene, USA, 631514). Using the AdEasy Adenoviral Vector System (Agilent Catalog #240009), the Flag-SREBP-1c cassette was cloned into a pShuttle-CMV vector. The shuttle vector was co-transformed into BJ5183 cells together with pAdEasy-1. Transformants were selected for kanamycin resistance and recombinants were produced in bulk using the XL10-Gold cell strain. Recombinant plasmid DNA was digested with PacI to expose the Inverted Terminal Repeat and transfected to HEK293 cells for posterior amplification and purification.

Primary hepatocyte isolation

Primary hepatocytes were isolated by perfusion of mouse livers with 40 ml buffer (5.5 mM KCl, 0.1% Glucose, 2.1 g/l $NaHCO_3$, 700 µM EDTA, 10 mM HEPES and 150 mM NaCl). After 20 minutes, the buffer was changed and the livers were infused with 50 ml collagenase buffer (5.5 mM KCl, 0.1% Glucose, 2.1 g/l $NaHCO_3$, 10 mM HEPES and 150 mM NaCl, 3.5 mM $CaCl_2$, 1% BSA, 500 µg/ml Collagenase Type I (300 u/mg)). Livers were perfused at a rate of 2 ml/min. Subsequently, livers were dissociated with the plunger of a syringe in 10 ml DMEM. The homogenate was filtered through a 100 µM cell strainer and collected. Hepatocytes were centrifuged at 100 *g* for 2 min and washed twice in DMEM containing 1x PenStrep. Next, cells were resuspended in hepatocyte medium. Cells were counted after staining with trypan blue (Thermo Fischer Scientific, USA, 15250061). Primary hepatocytes were seeded in rat tail collagen I (Sigma Aldrich, USA, C3867) coated 6-well dishes at a density of $6*10^5$ cells/well.

Blood Biochemistry

Plasma NEFA levels were analyzed using the NEFA kit HR Series NEFA-HR (2) (276-76491, 995-34791, 993-35191, 999-34691, 991-34891, WAKO Chemicals, Japan) according to manufactures instructions. Liver TG levels were measured from liver Folch extracts (67) using the Triglycerides FS 10 kit (Diasys, Germany, 15760991002). Samples were dissolved in 600 µl 1% Triton X-100.

Plasma insulin concentration was determined using the mouse Enzyme-linked Immunosorbent Assay (ELISA) test (Crystal Chem, USA # 90080). Plasma glucose concentration was measured from frozen plasma samples using a glucometer. In some cases, where only blood was available for glucose measurement, we used the conversion method described by D'Orazio, P*. et al.,* (68).

Fatty acid profile

Livers were homogenized, subjected to Folch extraction and lipids dried under nitrogen. Lipid extracts were pre-separated by thin layer chromatography (TLC). The band co-migrating with a triolein standard was scraped off and after addition of C15:0 as an internal standard, directly trans-esterified (1.2 ml toluene and 1 ml boron trifluoride-methanol (20%)) at 110 °C for 1 h. Gas Chromatography analysis of the corresponding FA methyl esters was performed as described (55) and concentrations were quantitated by peak area comparison with the internal standard.

Oil-Red-O staining

Oil-Red-O (Sigma-Aldrich, USA, O0625) was performed on 4% neutral buffered formalin, liver sections from mice were frozen in LN2 cooled methylbutane and samples were fixed and stained with ORO for later microscopic analysis.

Quantitative real-time Polymerase Chain Reaction (qPCR)

According to the protocol from RNA Cleanup Kit (NEB, T2030L), RNA was isolated from livers homogenized in Buffer M using Trizol (Invitrogen, USA, 15239794), cDNA prepared using High-Capacity cDNA Reverse Transcription Kit (Applied Biosystems, USA, 4368814) and qPCR performed using the SYBR Green Luna® Universal qPCR Master Mix (NEB, USA, M3003) on the QuantStudio™ 7 Flex Real-Time PCR System (Applied Biosystems™, USA, 4485701). Primers were designed with the NCBI primer designing tool (primer-blast) and are listed in supplementary table 1. Relative mRNA levels were analyzed as described by Schmittgen *et al.,* (69) with modifications, as follows. The relative PCR- efficiency of the gene of interest (GOI) primer sets compared to the 18s rRNA (HKG) primer set was determined by computational standard curve analysis in QuantStudio™ 7 Flex Software, Applied Biosystems™, USA) and subsequent division of GOI/HKG primer efficiencies. The resulting value was used as a base to compute relative gene expression using delta CT values.

Western Blotting

WB was performed using 4-20% SDS gels (Bio-Rad, 4561096) and blotted on 0.45 µm nitrocellulose membranes (GE healthcare, 15259794). Next, membranes were stained with Ponceau-S solution (Sigma Aldrich, USA, P7170) for protein load normalization and then blocked using skim milk powder (Sigma Aldrich, USA, 1153630500) /PBS/TWEEN® 20 (Sigma Aldrich, USA, P1379) (0.05,1,0.05; w/v/v). Membranes were incubated with specific primary antibodies. As secondary antibodies, respective horseradish peroxidase-coupled secondary antibodies were used. Signals were detected using the ChemiDoc Imaging System (Biorad, USA, 17001401). WB band intensities were analyzed using image J, NIH, software package (70). Relative levels of N-SREBP-1c were determined by the division of N-SREBP-1c band intensities through respective P-SREBP-1c band intensities. Insulin signaling WB were analyzed as the relative proportions of phosphorylated proteins / proteins. Membranes were incubated with the antibodies mentioned in the respective figures, which are described in detail in Supplementary Table 2.

Immunofluorescence (IF)

IF was performed and co-localization of GFP-SCAP and GM130 was analyzed, as previously described by Shao *et al*., (71). Hepatocytes were seeded at a confluence of $2.5*10^5$ into 6 well-plates in hepatocyte medium. Next day, hepatocytes were transfected with 1 µg pGFP-SCAP plasmid using Lipofectamine 2000 (Thermo Fisher, USA, 11668019). 48 h later, the cells were treated with 1% hydroxypropyl-beta-cyclodextrin (HPCD) to deplete sterols for 1 h in DMEM medium. Next, cells were supplemented with 5% LPDS medium plus the addition of 50 µM mevalonate and 50 µM mevastatin for 2 h or plus 2.5 µM 25-HC when indicated. Then, cells were washed with PBS, fixed in formaldehyde/PBS (0.03/1; w/v) at room temperature for 10 min, and permeabilized with Triton X-100/PBS/glycine (0.05/0.9/0.1; v/v/v) for 3 min at room temperature. Next, cells were incubated for 30 min with primary antibodies (anti-GFP and anti-GM130) and respective Alexa-488 (green) and Alexa-594 (red) coupled) secondary antibodies, followed by DAPI (Sigma Aldrich, USA, D9542) staining.

Samples were visualized using the Olympus BX51 microscope. Quantitative colocalization analysis was performed using 20 pictures per condition. The images were analyzed with Image J and the JACoP plug-in.

Ethical approval

All animal studies were performed in accordance with the guidelines and provisions of the Commission for Animal Experiments of the Austrian Ministry of Education, Science and Research (BMBWF). Approved animal applications and amendments include, BMBWF-66.007/0015-V/3b/2018; BMBWF-66.007/0004-V/3b/2019 and BMBWF-2020-0380.481.

Statistical analysis

Statistical significance was determined with Graph Pad Prism 8 using unpaired Student's t-test. All data represent mean values of the biological replicates ± standard error. Statistical analysis between 2 groups of biological replicates. Linear correlations were determined by Pearson’s correlation coefficient. (Holm Sidak method, alpha 0.05). Outlier analysis was performed using Grubb’s test. Each biological replicate was defined as a biological unit (e.g. a liver). If applicable, biological replicate values were calculated as the mean value of technical replicate values.

3. RESULTS

3.1 SREBP-1c hepatic activation is regulated by Adipose ATGL

As discussed in the introduction, SREBP-1c activation is highly dependent on nutritional status. In mice, P-SREBP-1c transcription is inhibited during fasting. Conversely, mice fed a diet with a high sugar content after prolonged fasting exhibit a significant increase in N-SREBP-1c activation. Therefore, to assess the effect of ATGL deletion in the adipose tissue on hepatic SREBP-1c regulation, we used Adipocyte-specific ATGL knockout (AAKO) mice (*Atgl*$^{flox/flox}$, *Adipoq-Cre*) or isogenic controls (*Atgl*$^{flox/flox}$) and performed fasting/refeeding experiments following the methodology described by Horton *et al* (30).

Groups of AAKO and control mice were fasted and then sacrificed (Fasted group) or fasted and then refed with a high carbohydrate diet (HCD), consisting of chow food supplemented with a high sugar content. To assess postprandial SREBP-1c regulation, the refed mice were sacrificed 3 h, 6 h, or 9 h after refeeding (Refed group). Liver resection was performed to isolate the microsomal membrane extracts (MM) and the soluble nuclear fraction (NEX), containing the precursor P-SREBP-1c and the transcriptionally active N-SREBP-1c forms, respectively, as depicted in the experimental scheme below (Figure 1A). The MM and NEX extracts were used to perform Western Blot (WB) to detect the P-SREBP-1c and N-SREBP-1c signals using SREBP-1c-specific antibodies.

The results evidenced that the P-SREBP-1c WB signal was undetectable during fasting but progressively increased after refeeding, showing a stronger precursor activation at the 9 h refed time point in both AAKO and controls groups (Figure 1B). The WB signals for N-SREBP-1c were densitometrically analyzed and normalized to protein loading as determined by Ponceau Staining, and N-SREBP-1c levels were quantified.

N-SREBP-1c was undetectable during fasting and 3 h after refeeding in both groups. However, 6 h after refeeding, N-SREBP-1c was strongly activated in the AAKO group compared to controls (Figure 1C). At the 9 h refed time point, the signals for N-SREBP-1c were equal in both groups (Figure 1C).

To further assess the effect of adipose ATGL deletion on SREBP-1c regulation, we analyzed the hepatic expression of various SREBP-1c target genes by Real-Time qPCR (RT-qPCR). Consistent with the SREBP-1c WB signals, *Fasn* and *Acaca* mRNA were significantly upregulated in AAKO mice during refeeding. Interestingly, *Srebf-1* expression was also upregulated during fasting and the 3 h refed timepoint in the AAKO group compared to controls (Figure 1D).

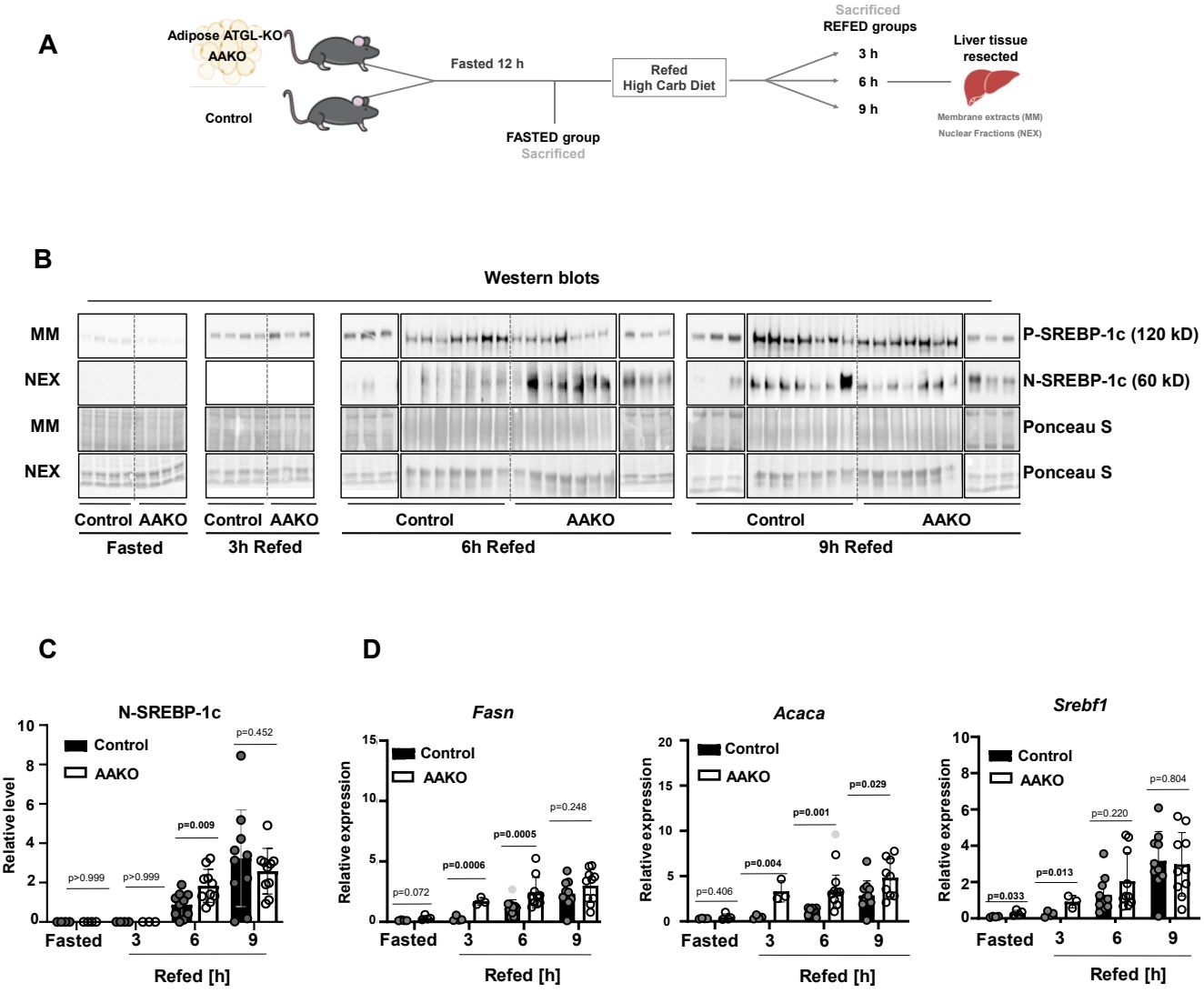

Figure 1: Adipose tissue ATGL regulates SREBP-1c in the liver. (A) Control and AAKO (Adipocyte-specific ATGL knockout) mice were fasted for 12h and then sacrificed (Fasted) or fasted and then refed a high carbohydrate diet (HCD) and sacrificed at different time points (Refed). The livers were used to obtain microsomal membrane fractions (MM) and nuclear extracts (NEX) that contained P-SREBP-1c and N-SREBP-1c, respectively. **(B)** Western Blots were performed using SREBP-1c antibody. Ponceau staining was used as loading control. Each lane corresponds to liver extracts from individual mice. The horizontal lines in the WB denote separate experiments. **(C)** Optical density was determined to calculate proteolytically cleaved N-SREBP-1c levels, which were normalized to Ponceau-S and presented in the graphs. **(D)** Liver *Fasn, Acaca and Srebf1* (mRNA) levels were analyzed by qPCR. Unpaired t-tests were performed (n=4-7 / group). Outliers are shown as light dots. *Adapted from (65)*

During fasting, ATGL-mediated lipolysis releases NEFAs from the adipose tissue into the circulation, which are then transported to the liver, where they are re-esterified and stored as TG. The analysis of NEFA species in plasma (Figure 2A) showed that AAKO mice displayed significantly lower plasma NEFA concentration during fasting than controls, especially from the uFA species (16:1, 18:1 and 18:2). In contrast, saturated FA (sFA) (16:0, and 18:0) did not show differences (Figure 2A). In line, liver NEFAs showed significantly lower 18:1 and 18:2 species content in the AAKO group (Figure 2B).

The analysis of total plasma NEFA during fasting and refeeding (Figure 2C) showed discrete variations at the 6h and 9h time points between the groups. The quantification of liver TG content showed significantly lower concentrations during fasting and at the 9 h refed timepoint in AAKO mice (Figure 2D). This was in line with the results from the histological analyses of the hepatic neutral lipid content during fasting, determined by Oil-Red-O staining (ORO), which revealed lower TG content in AAKO mice compared to controls (Figure 2E).

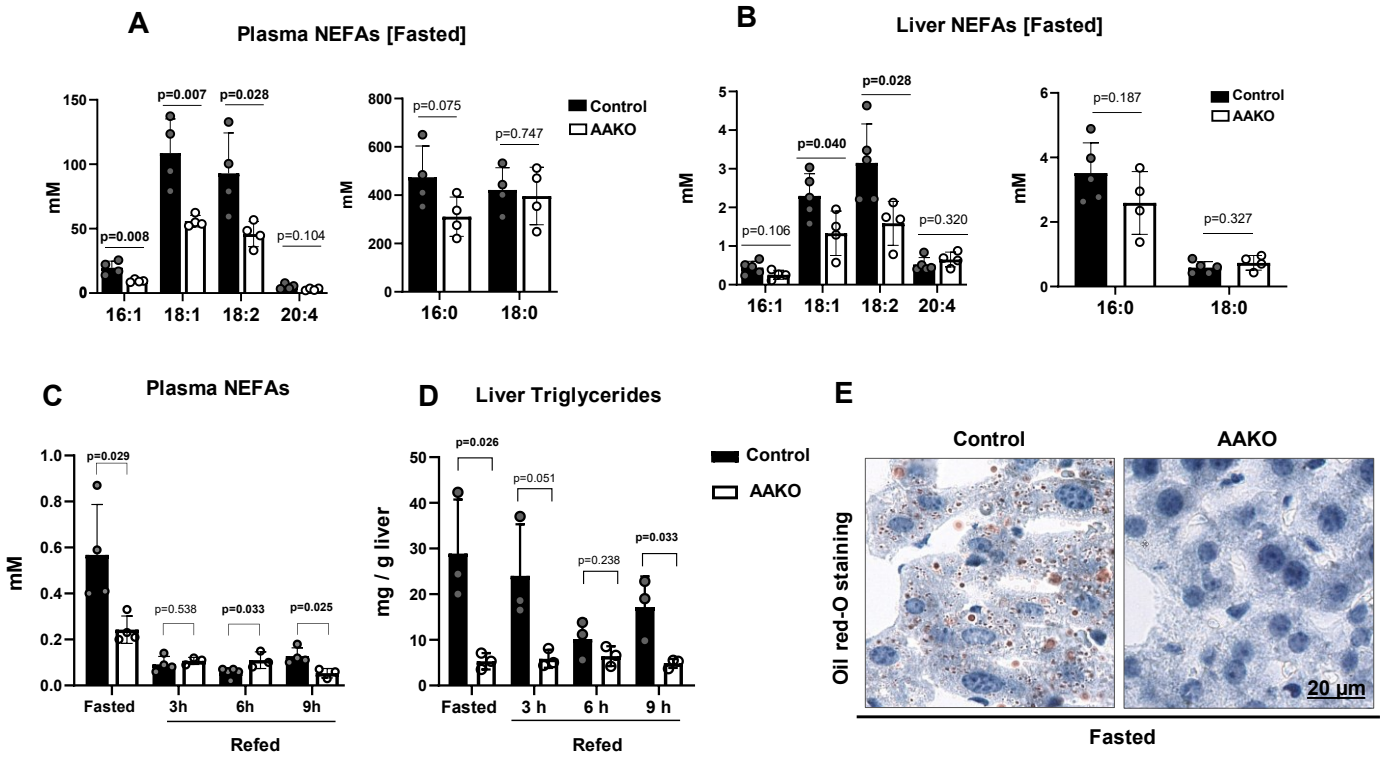

Figure 2: AAKO mice show lower plasma and liver NEFAs. Control and AAKO (Adipocyte-specific ATGL knockout) mice were fasted for 12h and then sacrificed (Fasted) or fasted and refed a high carbohydrate diet (HCD) and later sacrificed at different time points (Refed)**. (A)** Plasma NEFA (non-esterified fatty acids) and **(B)** liver NEFA levels were measured by GC/FID (Gas Chromatography-Flame Ionization Detection) during fasting, or **(C)** after refeeding n=4-10 / group. **(D)** Liver TG content was measured using GC/FID. n=3-5/group. **(E)** Histological visualization of neutral lipid content in the liver was performed by Oil-red-O staining in fasted Control and AAKO mice. Representative images are shown. Unpaired t-tests were performed (n=3-7 / group). *Adapted from (65)*

In addition, the analysis of plasma glucose levels showed no differences between the groups during the fasting or refeeding time course (Figure 3A). Furthermore, plasma insulin levels from 6 h and 9 h refed groups showed no significant differences between the genotypes (Figure 3B). To further analyze the role of insulin in SREBP-1c regulation, we analyzed a set of kinases involved in the insulin signaling pathway. For this purpose, the mouse liver extracts were subjected to WB to assess AKT and phospho-AKT (Ser473) activation, as well as Ser240/244 S6 and Ser235/236 S6 kinases from the p70S6K/S6 insulin pathway (Figure 3C). The results revealed a stronger activation of AKT after 9h refeeding in the AAKO group and significantly higher S6- phosphorylation at 6 h and 9 h refeeding compared to controls (Figure 3D).

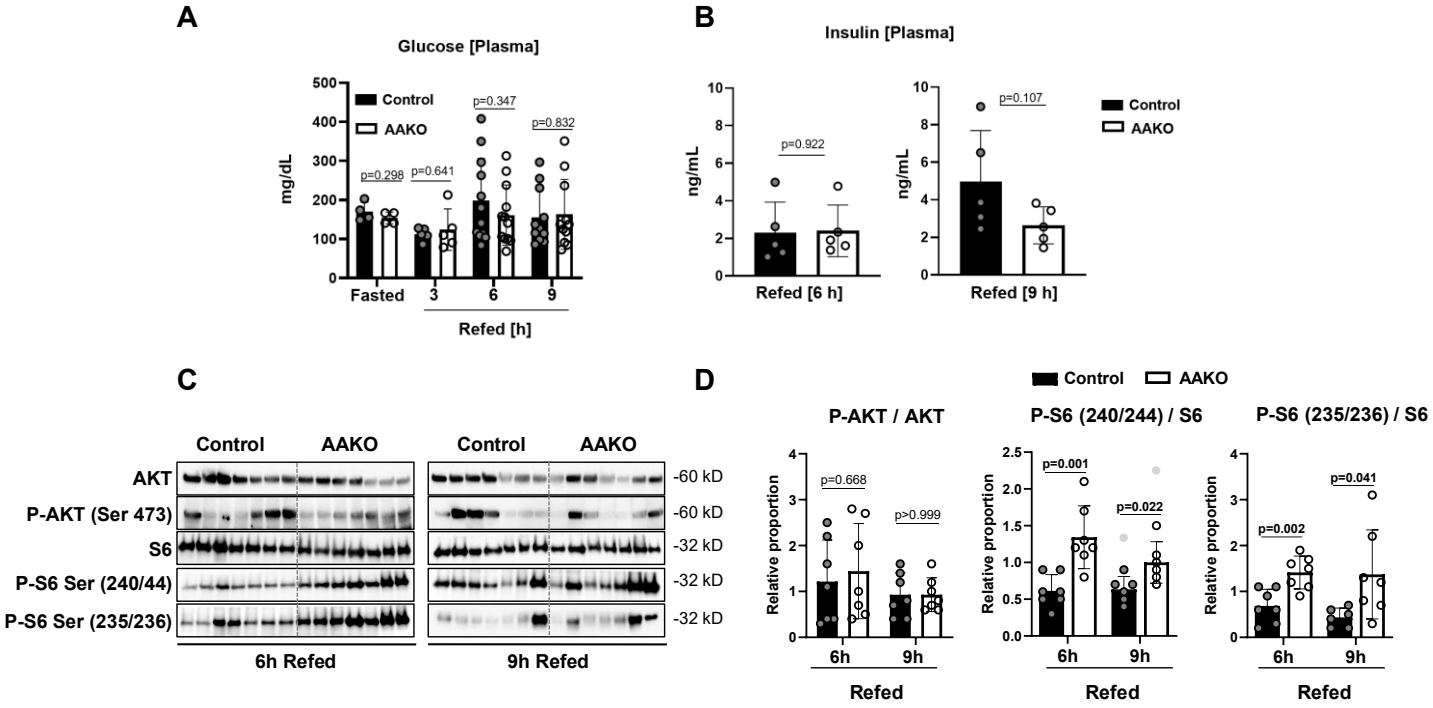

Figure 3. AAKO mice display higher insulin sensitivity. Control and AAKO (Adipocyte-specific ATGL knockout) mice were fasted for 12h and then sacrificed (Fasted) or fasted and refed a high carbohydrate diet (HCD) and later sacrificed at different time points (Refed). **(A)** Plasma glucose was measured using a glucometer. **(B)** Plasma insulin was determined by Enzyme-linked Immunosorbent Assay (ELISA). **(C)** WB were performed from total liver extracts to assess insulin signaling pathway using AKT/P-AKT, S6/P-S6 Ser 240/244 or P-S6 235/236 specific antibodies. **(D)** Relative proportions of phosphorylated proteins / proteins were calculated and presented in the graphs. Unpaired t-tests were performed (n=7 / group). Outliers are shown as light dots. *Adapted from (65)*

3.2 SREBP-1c hepatic activation is influenced by liver ATGL.

The liver is the central organ where the synthesis, uptake, and release of lipids take place. Therefore, we aimed to assess the role of liver ATGL lipolysis in hepatic SREBP-1c regulation. For this purpose, we used liver-specific ATGL-deficient ALKO mice (*Atgl*$^{flox/flox}$*, Alb-Cre*) and isogenic controls (*Atgl*$^{flox/flox}$).

Following the previous methodology (Figure 1A), groups of ALKO and control mice were fasted overnight and then sacrificed (Fasted group) or fasted and then refed with a HCD and sacrificed 3 h, 6 h, or 9 h after refeeding (Refed group), to assess SREBP-1c activation at different time points, as shown in the experimental scheme below (Figure 4A). The livers were resected and P-SREBP-1c and N-SREBP-1c signals were assessed by WB using SREBP-1c-specific antibodies.

The WB results showed that the P-SREBP-1c signal was very weak during fasting, but it gradually increased after refeeding in both groups (Figure 4B). A similar behavior was observed for the N-SREBP-1c signal; however, at the 6 h refed timepoint, ALKO mice showed significantly higher N-SREBP-1c levels determined by densitometrical analysis of the signal intensity (Figure 4C). In line, the *Srebf1* gene showed higher expression in ALKO mice livers during fasting, 3 h and 6 h after refeeding, while *Fasn* and *Acaca* expression showed an upregulation only at the 6 h timepoint compared to controls (Figure 4D).

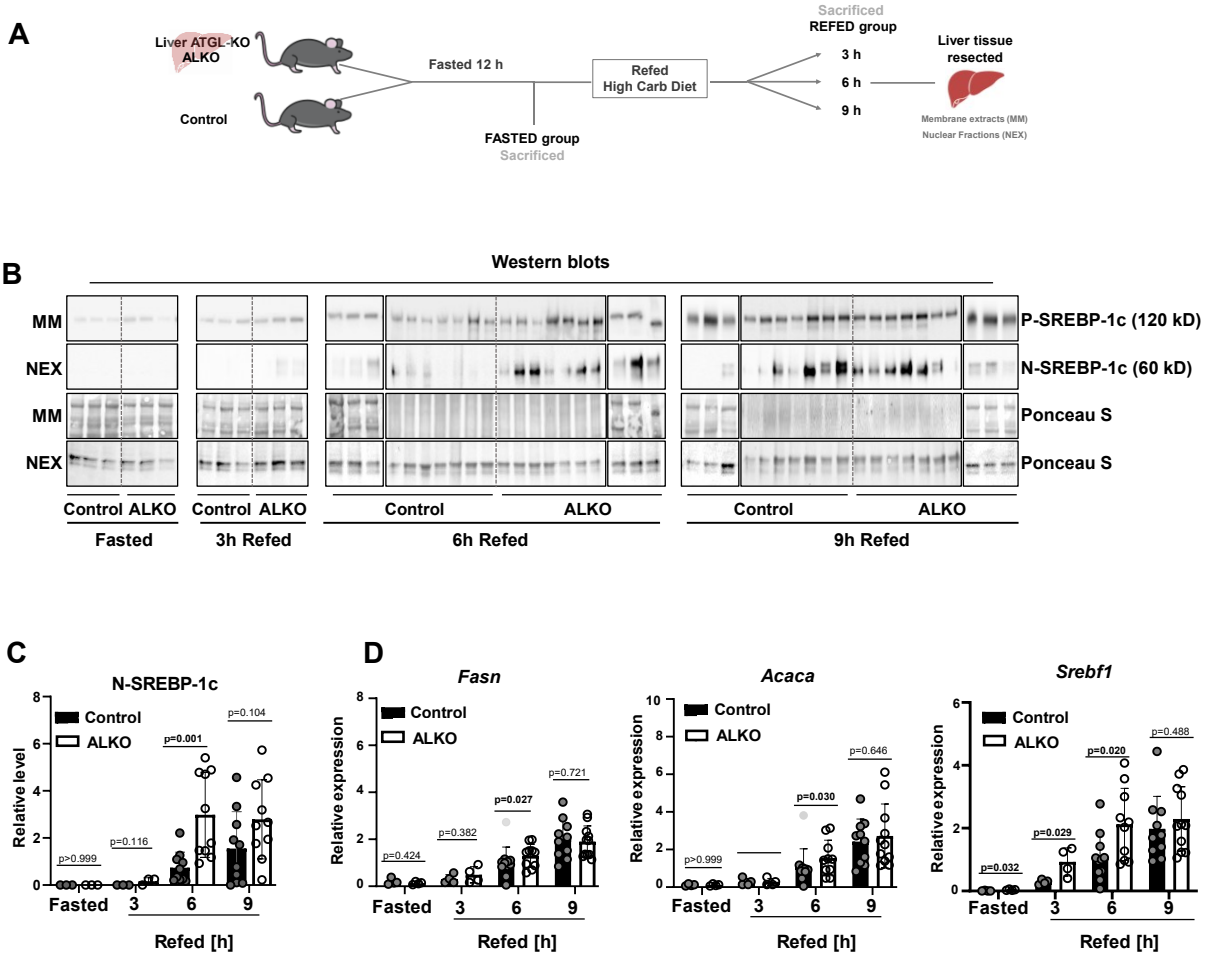

Figure 4: Hepatic SREBP-1c regulation in ALKO mice. (A) Control and ALKO (ATGL liver specific knockout) mice were fasted for 12 h and then sacrificed (Fasted) or fasted and then refed a high carbohydrate diet (HCD) and sacrificed at different time points (Refed). The livers were used to obtain microsomal membrane fractions (MM) and nuclear extracts (NEX) that contained P-SREBP-1c and N-SREBP-1c, respectively. **(B)** Western Blots were performed using SREBP-1c antibody. Ponceau staining was used as loading control. Each lane corresponds to liver extracts from individual mice. The horizontal lines in the WB denote separate experiments. **(C)** Optical density was determined to calculate proteolytically cleaved N-SREBP-1c levels, which were normalized to Ponceau-S and presented in the graphs. **(D)** Liver *Fasn, Acaca and Srebf1* (mRNA) levels were analyzed by qPCR. Unpaired t-tests were performed (n= 3-7 / group). Outliers are shown as light dots. *Adapted from (65)*

The analysis of fasting plasma NEFA concentrations revealed no differences between ALKO and control mice during fasting. This trend persisted in plasma NEFAs after refeeding a HCD (Figure 5A). Liver NEFA species determination by GC/FID showed a higher content of 16:1, 18:1 and 16:0 FA species in ALKO mice during fasting (Figure 5B). Liver TG content analysis showed consistently higher levels in AAKO mice compared to controls but only significant at the 6 h refed time point. (Figure 5C). Furthermore, the neutral lipid liver content determined by ORO staining showed a marked lipid accumulation during fasting in ALKO mice compared to the control group (Figure 5D).

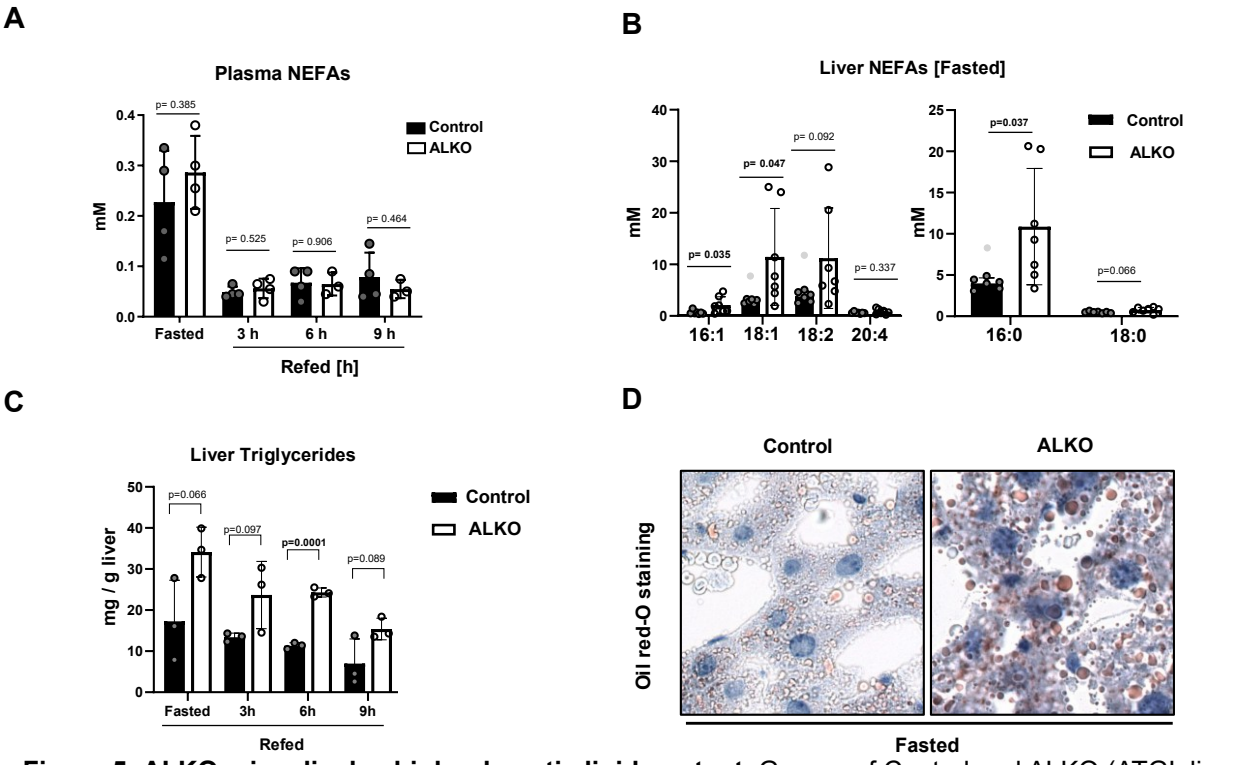

Figure 5: ALKO mice display higher hepatic lipid content. Groups of Control and ALKO (ATGL liver specific knockout) mice were fasted for 12h and then sacrificed (Fasted) or fasted and refed a high carbohydrate diet (HCD) and later sacrificed at different time points (Refed)**. (A)** Plasma NEFA (non-esterified fatty acids) and **(B)** Liver NEFA levels were measured by GC/FID (Gas Chromatography-Flame Ionization Detection) during fasting. **(C)** Liver TG content was measured using GC/FID. **(D)** Histological visualization of neutral lipid content in the liver was performed by Oil-red-O staining (ORO) in fasted Control and ALKO mice. Representative images are shown. Unpaired t-tests were performed (n=4-7/group). Outliers are shown as light dots. *Adapted from (65)*

In addition, the determination of plasma glucose (Figure 6A) or insulin concentration (Figure 6B) revealed no differences between ALKO and control groups. Furthermore, the analysis of the hepatic insulin signaling pathway determined by WB (Figure 6C), showed no changes in AKT/pAKT activation or S6 phosphorylation between the groups (Figure 6D),

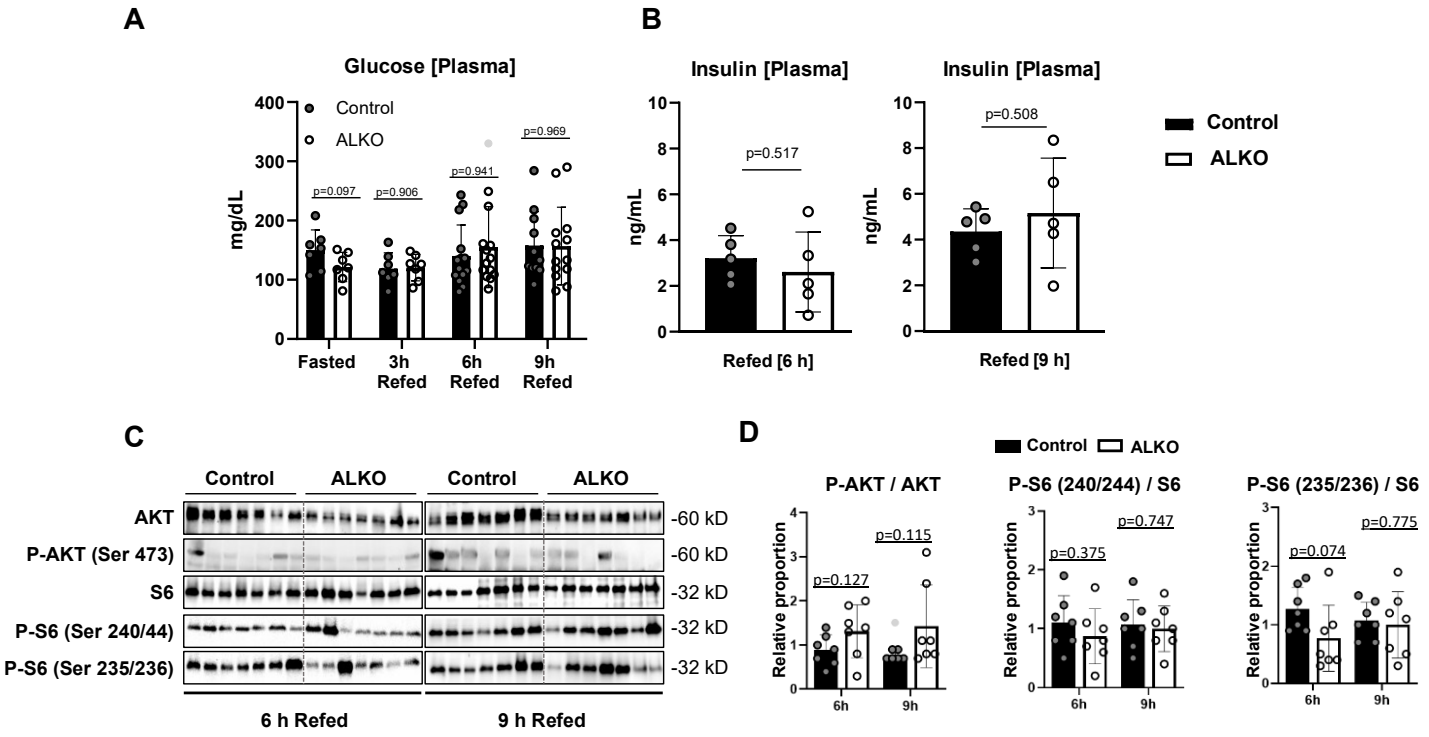

Figure 6. ALKO mice display normal insulin sensitivity. Groups of Control and ALKO (ATGL liver specific knockout) mice were fasted for 12h and then sacrificed (Fasted) or fasted and refed a high carbohydrate diet (HCD) and later sacrificed at different time points (Refed). **(A)** Plasma glucose was measured using a glucometer. **(B)** Plasma insulin was determined by Enzyme-linked Immunosorbent Assay (ELISA). **(C)** WB were performed from total liver extracts to assess insulin signaling pathway using AKT/P-AKT, S6/P-S6 Ser 240/244 or P-S6 235/236 specific antibodies. **(D)** Relative proportions of phosphorylated proteins / proteins were calculated and presented in the graphs. Unpaired t-tests were performed (n=4-7 / group). Outliers are shown as light dots. *Adapted from (65)*

3.3 *In vitro* SREBP-1c cleavage-activation is regulated by fatty acids.

Our findings showed that hepatic SREBP-1c was significantly upregulated in the absence of adipose or hepatic ATGL (Figure 1B and 4B). However, it was unclear if this effect was directly related to impaired ATGL lipolysis or due to SREBP-1c insulin activation after refeeding a HCD. Therefore, we wanted to elucidate further the direct role of ATGL-derived FA on SREBP-1c cleavage activation.

For this purpose, our group developed an SREBP-1c cleavage-activation reporter system that contained a Flag-tagged human *SREBF1* cDNA cassette (Flag-SREBP-1c) that was inserted into a vector, which contains a CMV promoter, allowing its constitutive expression. To test the system *in vitro*, we used the hepatic HepG2 cell line, which was transiently transfected with the Flag-SREBP-1c vector using lipofectamine. Two days after transfection, the cells were incubated in either lipoprotein-deficient serum (LPDS) to induce SREBP-1c activation (Lipid depleted) or in LPDS medium plus the addition of 100 μM of different albumin-bound FA (16:0,18:1, 18:2, 16:1 or 20:4) or with 25 hydroxycholesterol (25-HC), a potent SREBP cleavage activation inhibitor. Non-transfected HepG2 cells were used as a negative control (Figure 7A).

After 16 h of treatment, the cells were harvested, and whole cell extracts were used to detect Flag-SREBP-1c using an anti-Flag specific antibody by WB. The Flag-SREBP-1c allowed us to detect the precursor and nuclear SREBP-1c forms on the same membrane. However, the two signals were exposed separately for better visualization (Figure 7B). The N-SREBP-1c and P-SREBP-1c signal intensities were determined by densitometrical analysis. The relative levels of cleaved N-SREBP-1c were calculated as the fraction of N-SREBP-1c / P-SREBP-1c band intensities (Figure 7C).

Interestingly, the results demonstrated that under lipid-depleted conditions, SREBP-1c cleavage activation was induced, similar to the saturated FA 16:0 treatment. Conversely, when the cells were incubated in LPDS plus the addition of different uFA

species or plus 25-HC, N-SREBP-1c relative levels were strongly suppressed, confirming that our SREBP-1c cleavage reporter vector was regulated by FAs and sterols (Figure 7C) (6, 13, 26, 44).

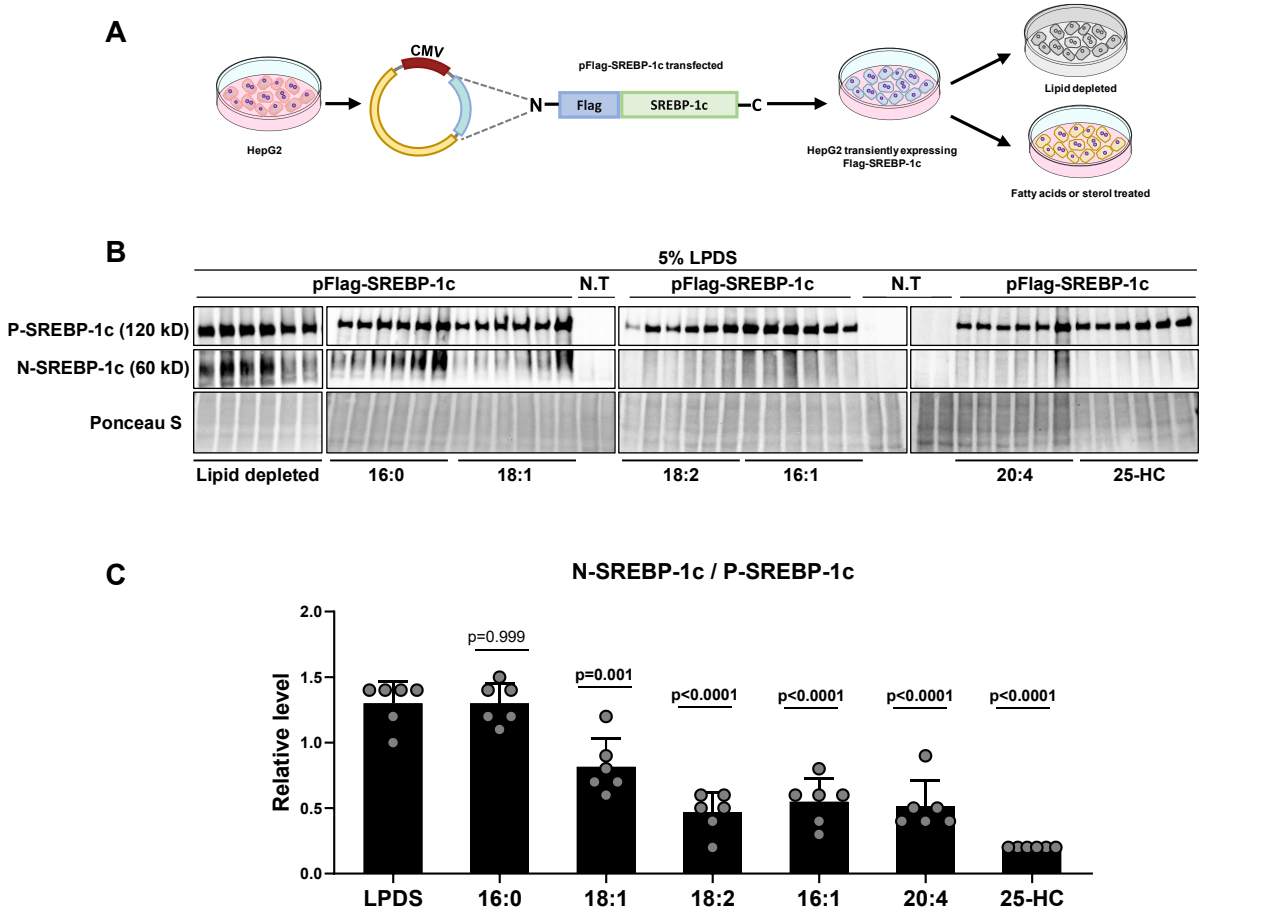

Figure 7. Establishment of Flag-SREBP1c cleavage reporter vector *in vitro*. (A) Our group developed a Flag-SREBP-1c vector that contains the human triple Flag-tagged *SREBF1* cDNA (Flag-SREBP-1c) expressed under a CMV promoter, which was transfected into the HepG2 hepatic cell line, by Lipofectamine transfection. **(B)** Two days later, the cells were incubated in 5% LPDS (lipoprotein deficient serum) (lipid depleted group), or 5% LPDS plus supplementation with 100 µM of different fatty acids (16:0, 18:1, 18:2, 16:1 or 20:4) and treated for 16h. Cells treated with 25-hydroxycholesterol (25-HC) were used as SREBP-1c suppression control. Non transfected cells (N.T) were used as transfection control. Whole cell extracts were collected and used to analyze Flag-SREBP-1c cleavage activation by Western blot (WB) using anti-Flag specific antibody. Each WB lane represents a single treated well. **(C)** Optical densitometry was measured to calculate the relative levels of cleaved Flag-N-SREBP-1c, which are represented in the graph. Unpaired t-tests were used to calculate significance levels (n=6/group). *Adapted from (65)*

3.4 SREBP-1c cleavage-activation is regulated by fatty acids *in vivo*.

After confirming that our Flag-SREBP-1c vector was able to track SREBP-1c cleavage activation *in vitro* and that uFAs could suppress Flag-N-SREBP-1c activation, we sought to establish the same system *in vivo*. Therefore, to express the Flag-SREBP-1c cleavage reporter system in mouse livers, we cloned the previously described human Flag-tagged-*SREBF1* into an adenoviral vector using the AdEasy system, resulting in the Ad-Flag-SREBP-1c vector.

To test the SREBP-1c cleavage reporter system *in vivo*, we injected $2x10^9$ PFU (plaque forming units) of Ad-Flag-SREBP-1c via tail vein injection into C57BL/6J wild-type mice. The mice were treated four days after transduction to reach stable adenoviral expression. Next, we performed the previously described fasting/refeeding experiments to track SREBP-1c cleavage activation. The mice were fasted for 12 h overnight and sacrificed (Fasted group) or fasted and refed a HCD overnight and then sacrificed (HCD group), as depicted in the experimental scheme below (Figure 8A). The livers were excised, and MM and NEX extracts were isolated to detect Flag-tagged P-SREBP-1c and N-SREBP-1c by WB using an anti-Flag specific antibody.

Interestingly, the results showed that fasted and HCD mice groups displayed similar Flag-P-SREBP-1c expression, confirming the constitutive expression of our vector. Conversely, the Flag-N-SREBP-1c signals showed a marked difference between the fasted and HCD groups. N-SREBP-1c was inactive in the fasted group, despite stable P-SREBP-1c expression (Figure 8B). However, the HCD group showed significantly higher induction of Flag-N-SREBP-1c cleavage activation, determined by the N-SREBP-1c/P-SREBP-1c ratio (Figure 8C). In line with these results, the mRNA expression of the SREBP-1c target genes *Fasn*, *Acaca* and *Srebf1* showed a significant upregulation in the HCD group compared to the control group (Figure 8D).

Moreover, the determination of plasma glucose and insulin concentration showed a strong increase after HCD compared to fasting (Figure 8E). Additionally, the WB analysis of the kinases involved in the insulin activation pathway (Figure 8F), showed strong pAKT/ AKT and S6/Ser 240-244 activation in the livers of HCD-fed mice (Figure 8G). The determination of plasma NEFA composition by by GC/FID showed higher unsaturated NEFAs (16:1, 18:2, 18:3 and 20:4) in fasted mice compared to the HCD fed group (Figure 8H).

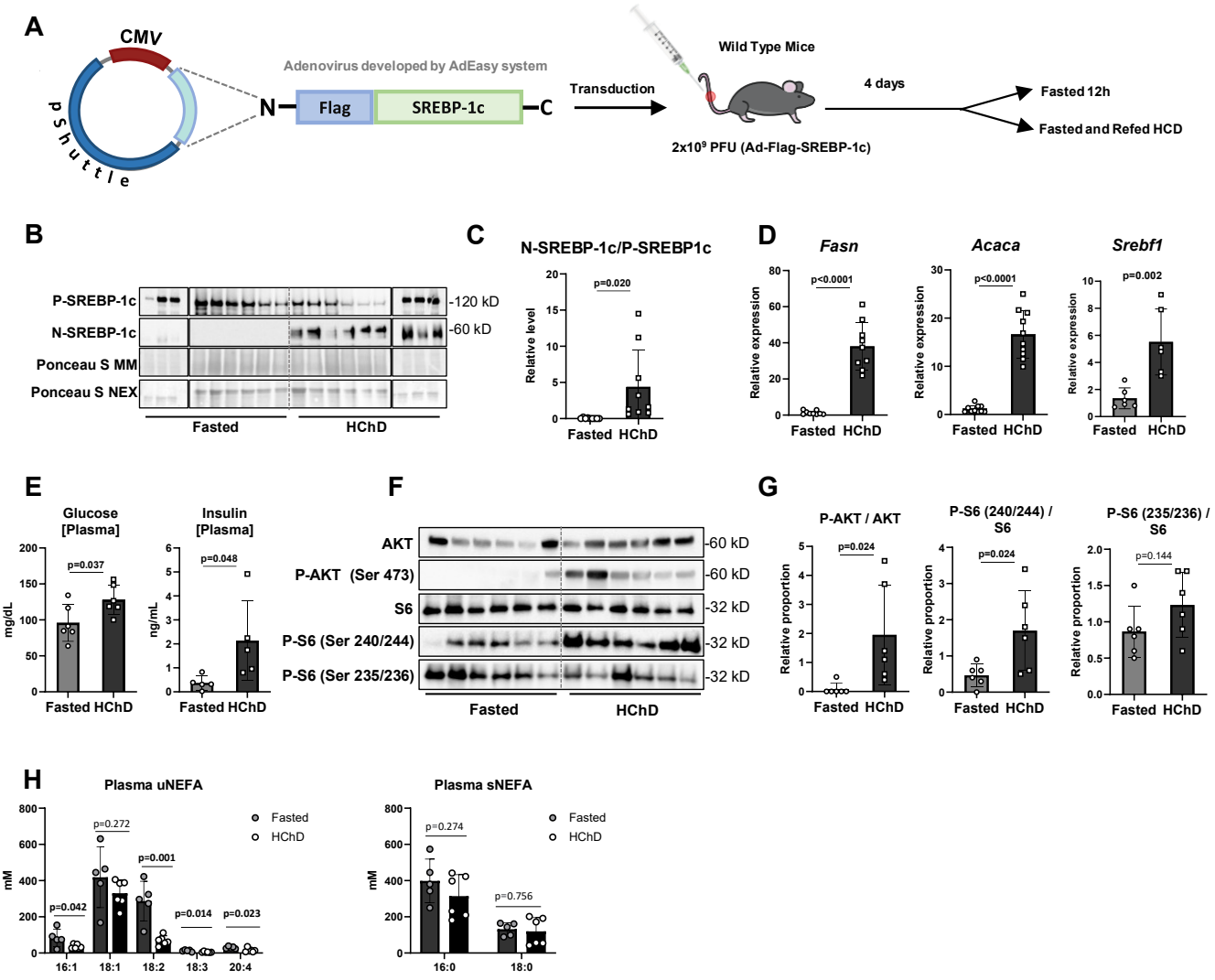

Figure 8. Establishment of Flag-SREBP1c cleavage reporter vector *in vivo*. (A) The Flag-SREBP-1c cassette was cloned into a shuttle vector that contains a CMV promoter, resulting in the Ad-Flag-SREBP-1c cleavage reporter vector, using the AdEasy system. Wild type mice were transduced with $2x10^9$ PFU Ad-Flag-SREBP-1c. Four days later, mice were either fasted overnight (Fasted) or fasted and refed a high carbohydrate diet (HCD) overnight. **(B)**The mice were sacrificed and livers resected to obtain microsomal membrane fractions (MM) and nuclear extracts (NEX) that contained the Flag P-SREBP-1c and Flag N-SREBP-1c, respectively, and subjected to Western blot (WB) using anti-Flag antibody. Each lane corresponds to liver extracts from individual mice. **(C)** Optical density of N-SREBP-1c and P-SREBP-1c was determined to calculate relative levels of proteolytically cleaved N-SREBP-1c, which were normalized to Ponceau-S and presented in the graphs. **(D)** Liver *Fasn*, *Acaca* and *Srebf1* (mRNA) levels were determined by qPCR (quantitative real-time Polymerase Chain Reaction). **(E)** Plasma glucose was measured using a glucometer. Plasma insulin was determined by Enzyme-linked Immunosorbent Assay (ELISA). **(F)** WB was performed from total liver extracts to assess insulin signaling pathway using AKT/P-AKT, S6/P-S6 Ser 240/244 or P-S6 235/236 specific antibodies. **(G)** Relative proportions of phosphorylated proteins / proteins were calculated and presented in the graphs. **(H)** Plasma NEFA (non-esterified fatty acids) levels were measured by GC/FID (Gas Chromatography-Flame Ionization Detection). Unpaired t-tests were used to calculate significance levels (n=5-6/group). *Adapted from (65).*

Once the AdFlag-SREBP-1c reporter system was established *in vivo*, we sought to test if the dietary FA composition modulated our SREBP-1c cleavage reporter vector in the liver. Therefore, wild-type mice were transfected with $2x10^9$ PFU of AdFlag-SREBP-1c vector. Four days later, the mice were given an uFA-rich diet, which consisted of chow food enriched with a high content of flaxseed oil, which has a predominant composition of α-linolenic acid (18:3). The second group was fed with a sFA-rich diet, which contained a high amount of saturated palmitic acid (16:0). Both groups were fed with the special diets for 3 consecutive days, in which the mice had free access to the food (Figure 9A). Later, the mice were sacrificed, and their livers were resected to analyze hepatic Flag-P-SREBP-1c and Flag-N-SREBP-1c cleavage activation.

Interestingly, our results showed that uFA-rich and sFA-rich diets exhibited similar WB signal intensities of Flag-P-SREBP-1c (Figure 9B). However, when we analyzed the Flag-N-SREBP-1c/P-SREBP-1c ratio, the sFA-rich diet led to a significant upregulation of Flag-N-SREBP-1c compared to the uFA-rich diet group, as observed in the N-SREBP-1c/P-SREBP1c graph (Figure 9C). The analysis of SREBP-1c target genes only showed a significant upregulation in *Fasn* mRNA expression in the sFA diet group (Figure 9D).

Furthermore, plasma glucose analysis revealed similar concentrations in both groups, while plasma insulin levels were slightly higher in the sFA-rich diet group (Figure 9E). The analysis of the insulin activation pathway by WB showed no differences between the treatments (Figure 9F and 9G).

In addition, the determination of plasma NEFA composition confirmed a significantly higher 18:3 plasma NEFA concentration in mice fed an uFA-rich diet. Conversely, a higher concentration of 16:0 plasma NEFA was detected in the sFA diet group (Figure 9H), which was a product of the diet composition.

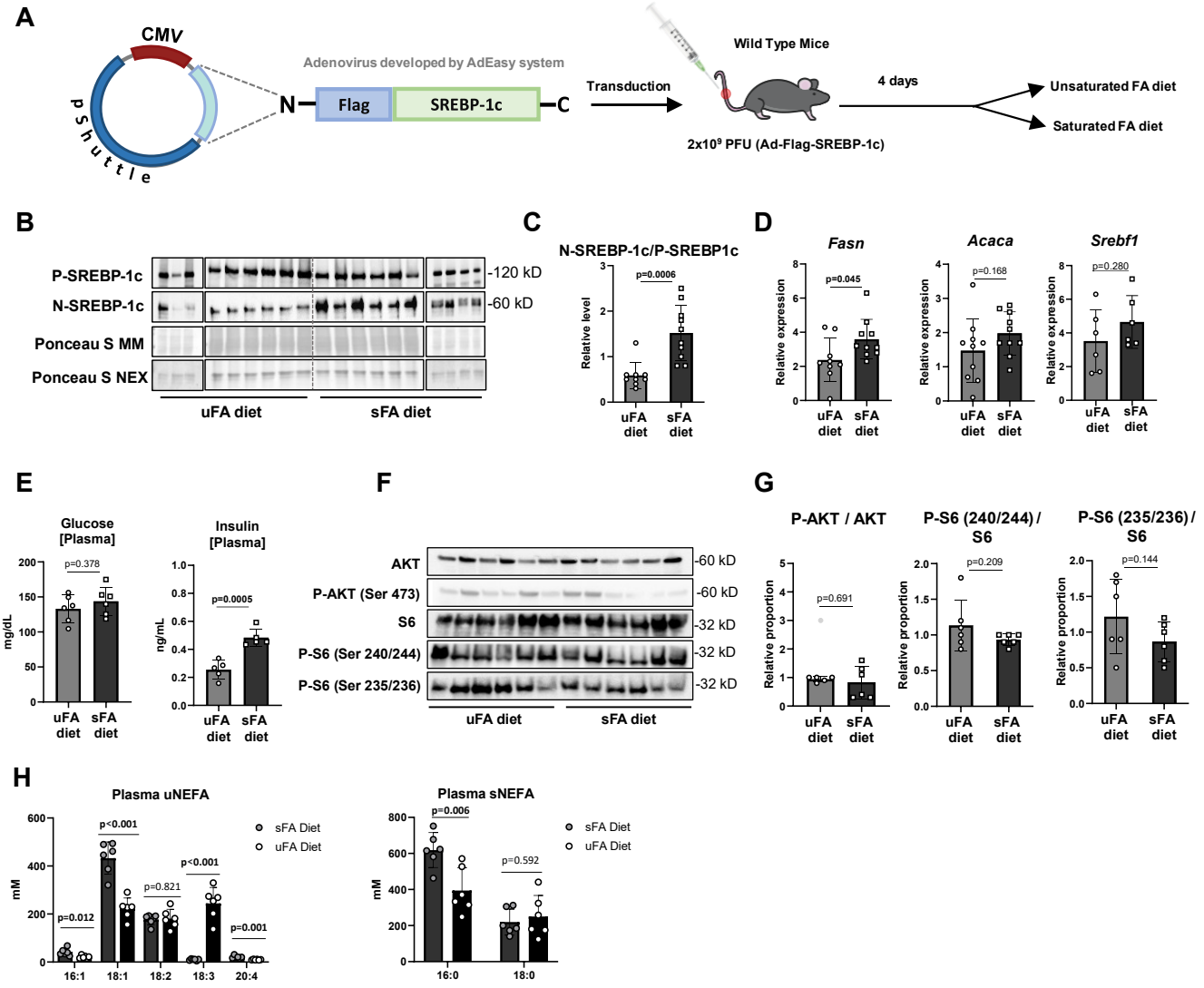

Figure 9. Flag-SREBP1c cleavage reporter is regulated by dietary fatty acids *in vivo*. (A) Wild type mice were transduced with 2x10^9 PFU AdFlag-SREBP-1c. Four days later, mice were treated with an unsaturated fatty acid rich diet (uFA diet), supplemented with flaxseed oil, or a saturated fatty acid rich diet (sFA diet), supplemented with palm oil, and fed for three consecutive days. **(B)** The mice were sacrificed and livers resected to obtain microsomal membrane fractions (MM) and nuclear extracts (NEX) that contained the Flag P-SREBP-1c and Flag N-SREBP-1c, respectively, and subjected to Western blot (WB) using anti-Flag antibody. Each lane corresponds to liver extracts from individual mice. **(C)** Optical density of N-SREBP-1c and P-SREBP-1c signal intensities was determined to calculate relative levels of proteolytically cleaved N-SREBP-1c, which were normalized to Ponceau-S and presented in the graphs. **(D)** Liver *Fasn*, *Acaca* and *Srebf1* (mRNA) levels were determined by qPCR (quantitative real-time Polymerase Chain Reaction). **(E)** Plasma glucose was measured using a glucometer. Plasma insulin was determined by Enzyme-linked Immunosorbent Assay (ELISA). **(F)** WB was performed from total liver extracts to assess insulin signaling pathway using AKT / P-AKT, S6 / P-S6 Ser 240/244 or P-S6 235/236 specific antibodies. **(G)** Relative proportions of phosphorylated proteins / proteins were calculated and presented in the graphs. **(H)** Plasma NEFA (non-esterified fatty acids) levels were measured by GC/FID (Gas Chromatography-Flame Ionization Detection). Unpaired t-tests were used to calculate significance levels (n=5-6/group). *Adapted from (65)*

3.5 Hepatic SREBP-1c cleavage-activation is suppressed by lipolysis-derived uFAs.

Our results showed that AAKO and ALKO mice displayed a significant N-SREBP-1c upregulation compared to controls after refeeding a HCD (Figure 1B and 4B). Interestingly, AAKO mice showed significantly lower plasma and liver uNEFAs during fasting (Figure 2A and 2B).To investigate the regulation in further detail, we wanted to test if uFAs derived from adipose tissue lipolysis are able to directly regulate hepatic SREBP-1c activation. For this purpose, we used our established SREBP-1c cleavage-reporter vector.

To test our hypothesis, Ad-Flag-SREBP-1c was transduced into groups of AAKO and control mice. Four days after transduction, both groups were fasted overnight and sacrificed the next morning (Figure 10A). The livers were excised and MM and NEX fractions were isolated to detect Flag-P-SREBP-1c and Flag-N-SREBP-1c by WB using an anti-Flag antibody (Figure 10B).

Interestingly, the WB results showed that fasted AAKO and control mice displayed stable Flag-P-SREBP-1c levels due to the constitutive expression of the vector. Remarkably, higher Flag-N-SREBP-1c levels were observed in AAKO mice livers during fasting (Figure 10C). Additionally, the expression of SREBP-1c target genes determined by qPCR revealed that *Fasn* was significantly upregulated in the livers of AAKO mice during fasting. However, no differences in *Srebf1* and *Acc1* expression were found between the groups (Figure 10D).

The analysis of plasma NEFAs showed significantly lower 16:1 and 18:1 content in AAKO mice compared to control during fasting, but no significant differences in other NEFA species (Figure 10E).

The determination of plasma glucose and insulin showed lower concentrations in AAKO mice during fasting than in controls (Figure 11A). To examine whether insulin influences Flag-SREBP-1c activation during fasting, we analyzed the insulin signaling pathway by WB, which showed that p-AKT and Ser-235/236 were not detectable during fasting in both groups (Figure 11B). However, the analysis of Ser-240/244 showed similar activation in both groups (Figure 11C).

To test if the exogenous supply of uFAs could influence the observed N-SREBP-1c upregulation in AAKO mice during fasting, we repeated the experiment (Figure 10A). Groups of AAKO and control mice were again fasted overnight; however, this time, the mice were injected with bovine serum albumin (BSA) complexed oleic acid (18:1), which was supplied via tail vein injection every 3h during the 12 h fasting period. Later, the mice were sacrificed, and their livers were resected to analyze Flag-P-SREBP-1c and Flag-N-SREBP-1c signals by WB.

Surprisingly, after we supplied the mice with exogenous oleic acid, the previously observed upregulation of Flag-N-SREBP-1c in AAKO mice was prevented. Consequently, the AAKO group exhibited a similar SREBP-1c cleavage-activation rate compared to control mice during fasting (Figure 10B and 10C). Additionally, the mRNA expression of SREBP-1c target genes *Fasn*, *Srebf1* and *Acc1* showed no differences between the groups after 18:1 infusion (Figure 10D).

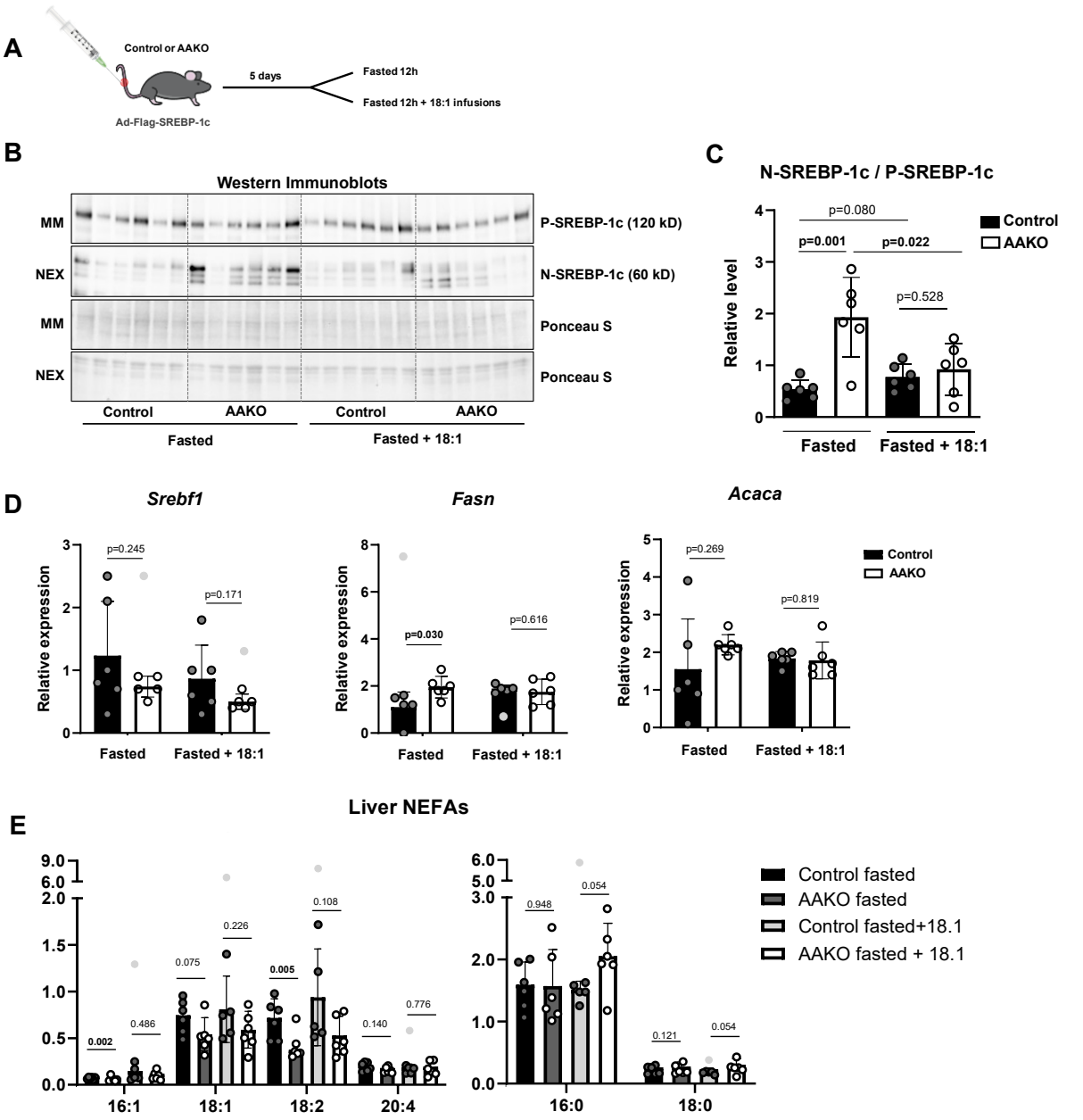

Figure 10. Unsaturated Fatty Acids inhibit SREBP-1c upregulation *in vivo*. (A) Adipocyte-specific ATGL knockout (AAKO) or Control mice were transduced with 2x10^9 PFU AdFlag-SREBP-1c. Four days later, the mice were fasted 12 h overnight (Fasted) or fasted and intravenously injected with Bovine Serum Albumin (BSA)-complexed oleic acid (18:1) 3 and 9 hours after initiating the fasting period. **(B)** The mice were sacrificed and livers resected to obtain microsomal membrane fractions (MM) and nuclear extracts (NEX) that contained the Flag P-SREBP-1c and Flag N-SREBP-1c, respectively, and subjected to WB using anti-Flag antibody. Each lane corresponds to liver extracts from individual mice. **(C)** Optical density of N-SREBP-1c and P-SREBP-1c signal intensities was determined to calculate relative levels of proteolytically cleaved N-SREBP-1c, which were normalized to Ponceau-S and presented in the graphs. **(D)** Liver *Fasn*, *Acaca* and *Srebf1* (mRNA) levels were determined by qPCR (quantitative real-time Polymerase Chain Reaction). **(E)** Liver NEFA levels were measured by GC/FID (Gas Chromatography-Flame Ionization Detection). Unpaired t-tests were used to calculate significance levels (n=6/group). Outliers are shown as light dots. *Adapted from (65)*

Furthermore, to analyze the glucose and insulin regulation on SREBP-1c, we determined the plasma glucose and insulin concentration, which showed no appreciable differences between the groups after exogenous supply of oleic acid (Figure 11 A). Furthermore, the analysis of the insulin activation pathway by WB showed that p-AKT and Ser-235/236 remained undetectable after 18:1 infusion in both groups (Figure 11B). However, S6/Ser-240/44 phosphorylation was active in both genotypes, compared to fasted mice, but no differences were found between the groups (Figure 11C).

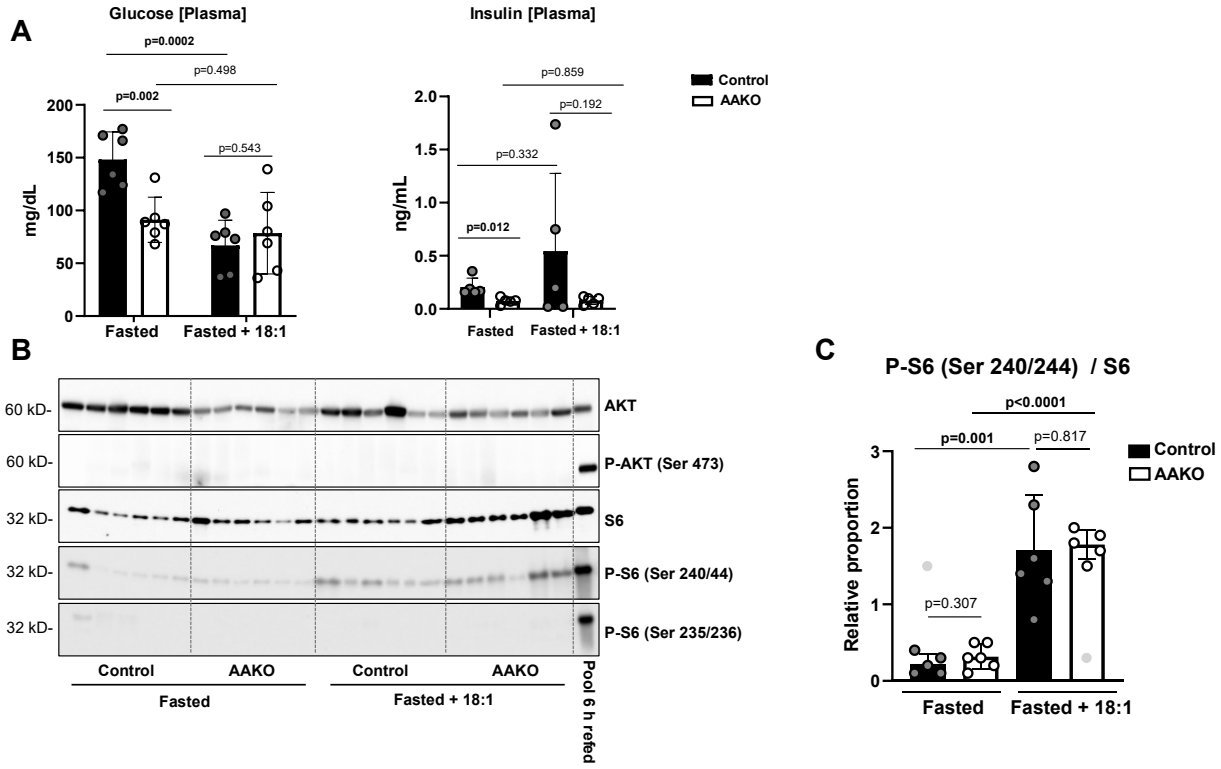

Figure 11. Insulin regulation in AAKO mice during fasting. Adipocyte-specific ATGL knockout (AAKO) or Control mice were transduced with 2x10^9 PFU AdFlag-SREBP-1c. Four days later, the mice were fasted 12 h overnight (Fasted) or fasted and intravenously injected with Bovine Serum Albumin (BSA)-complexed oleic acid (18:1) after 3 and 9 hours after initiating the fasting period (See Figure 10 A). **(A)** Plasma glucose was measured using a glucometer. Plasma insulin was determined by Enzyme-linked Immunosorbent Assay (ELISA). **(C)** WB was performed from total liver extracts to assess insulin signaling pathway using AKT / P-AKT, S6 / P-S6 Ser 240/244 or P-S6 235/236 specific antibodies. A pool of 3 liver extracts from Control mice refed a HCD and sacrificed at 6 h timepoint, was used as positive control (Pool 6 h refed). **(D)** Relative proportions of phosphorylated proteins / proteins were calculated and presented in the graphs. Unpaired t-tests were used to calculate significance levels (n=6/group). Outliers are shown as light dots. *Adapted from (65)*

3.6 uFAs suppress ER to Golgi transport in primary hepatocytes.

The experiments using the Flag-SREBP-1c cleavage reporter vector showed that uFAs inhibited hepatic SREBP-1c cleavage activation in AAKO mice. Moreover, we wanted to explore if this effect was regulated through the ER-Golgi transport mediated by the SREBP chaperone, SCAP(25).

For this purpose, we used a GFP-SCAP construct created by Shao *et al.,* (71) which allowed us to trace the ER to Golgi SCAP trafficking. Primary hepatocytes were isolated from C57/BJ6 mice and transfected with the GFP-SCAP plasmid. The next day, the cells were lipid-depleted using HPCD [(2-hydroxypropyl)-beta-cyclodextrin] and either incubated in Lipoprotein Deficient Serum (LPDS) medium (Lipid depleted group) or LPDS plus the addition of 2.5 μM of 25-HC or 100 μM of unsaturated 18:1 FA or saturated 16:0 FA.

After 16 h treatment, co-immunofluorescence microscopy (co-IF) was performed using anti-GFP and anti-GM130 (Golgi-marker) antibodies (Figure 12A). SCAP-GFP/GM-130 co-localization was determined by Pearson's correlation coefficient for each condition. The results demonstrated that 25-HC treatment reduced the SCAP transport to the Golgi, determined by a lower GFP-SCAP/GM130 co-localization, compared to the lipid-depleted condition. Importantly, the primary hepatocytes treated with 18:1 unsaturated fatty acid showed a significant decrease in GFP-SCAP/GM130 co-localization compared to 16:0 treatment or lipid depletion (Figure 12B). However, the treatment with 16:0 showed no effect on SCAP transport compared to the lipid-depleted condition (Figure 12B).

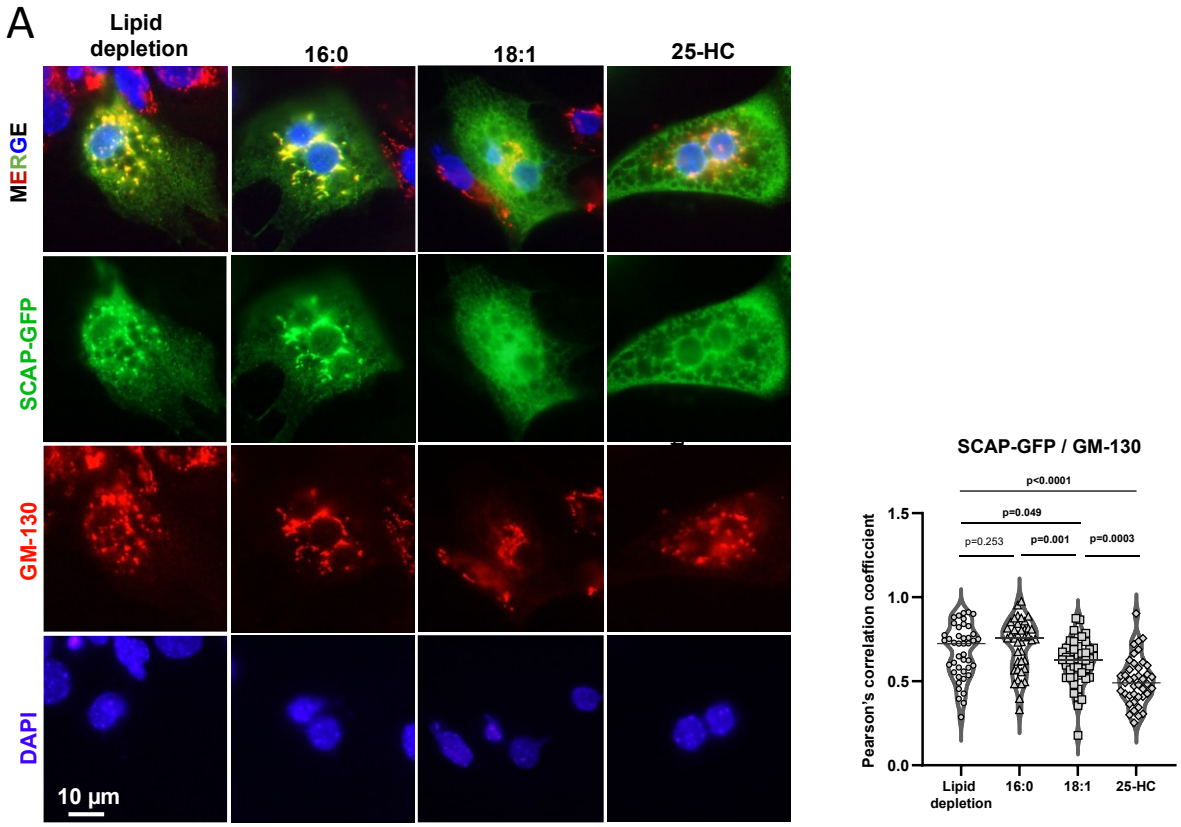

Figure 12: Unsaturated Fatty Acids suppress SCAP-SREBP-1c transport to the Golgi (A) Primary hepatocytes from wild type mice were isolated. The next day, cells were transfected with GFP-SCAP plasmid. Two days after transfection, the cells were treated with 1% w/v HPCD ([(2-hydroxypropyl)-beta-cyclodextrin]) for 1 h. Then, cells were either incubated in 5% Lipoprotein Deficient Serum (LPDS) medium with mevalonate and mevastatin (lipid depleted) or incubated in LPDS plus the addition of 2.5 µM of 25- hydroxycholesterol (25-HC) or plus 100 µM 16:0 or 18:1 FA. After two hours of treatment, the cells were fixed with formaldehyde and permeabilized with Triton X-100. GFP-SCAP was observed by immunofluorescence using anti-GFP and Alexa488 coupled secondary antibodies (green); Golgi was visualized using anti-GM130 and Alexa594 coupled secondary antibody (red); DAPI was used for nuclear staining. **(E)** SCAP-GFP/GM-130 colocalization was calculated by Pearson's correlation coefficient and represented in the violin plot. Unpaired t-tests were used to compute significance levels (n=40-46 cells/ group). *Taken from (65)*

4. DISCUSSION

Cardiovascular and metabolic diseases currently constitute the leading causes of death worldwide and represent a burden for the health of individuals and a big challenge for health systems all over the world. Although genetic factors significantly influence the development of these pathologies, their progression is closely related to nutrition. The influence of environmental factors such as a sedentary lifestyle and a prolonged over-nutrition state, mainly characterized by a high intake of saturated fats and simple carbohydrates, accelerates their development (7) (8).

Therefore, highly regulated biochemical and molecular pathways are needed to preserve cellular and energetic homeostasis. The adipose tissue and the liver are the primary tissues involved in energy metabolism and represent the principal FA source in the organism. Under high-energy demand, adipose tissue releases FA from the TG stored in cellular lipid droplets to be used as energy substrates through lipolysis, which is mainly regulated by ATGL. On the other hand, SREBP-1c is the master transcription factor that controls endogenous FA synthesis in the liver, where lipogenesis, lipid transport and catabolism take place.

In consequence, disorders in FA mobilization and synthesis lead to diverse metabolic disturbances. Evidence shows that SREBP-1c chronic over-activation induces lipid-mediated cellular stress that is related to the development of insulin resistance, obesity, diabetes mellitus, hepatosteatosis, dyslipidemias and atherosclerosis (9, 27) (72).

On the other hand, the mutations in the *Atgl* gene in humans lead to the development of cardiomyopathy and NLSD (1). Mouse models systemically lacking *Atgl* develop cardiac dysfunction as a result of the excessive accumulation of TG in the heart, which leads to premature death (60). Additionally, they also show a variety of metabolic disorders such as lipid accumulation, cold intolerance, disrupted β-oxidation, alterations in insulin sensitivity, hepatic steatosis, myopathy and impaired lipolysis (10).

Interestingly, adipocyte-specific ATGL knockout (AAKO) mice exhibit significantly lower uFA levels in plasma, as a consequence of disrupted lipolysis (55) (60). Remarkably, studies *in vitro* have shown that uFAs inhibit SREBP-1c cleavage activation (44) (45) (6). Furthermore, *Schoiswohl et al.*, evidenced that AAKO mice show significantly lower *Srebf1* mRNA levels in the adipose tissue, suggesting a link between ATGL lipolysis and SREBP-1c regulation (61).

However, to date, lipolysis and lipogenesis are considered metabolic processes regulated by independent mechanisms. To our knowledge, no studies have investigated the potential interaction between these pathways, which are regulated by ATGL and SREBPs, respectively (27). Therefore, in the present work, we focused on studying the potential regulatory role of FAs derived from ATGL lipolysis on SREBP-1c hepatic lipogenesis.

To test our hypothesis, we used two different ATGL knockout mouse models: Adipocyte-specific ATGL knockout (AAKO) (61) and liver-specific ATGL-KO mice (ALKO) (62), because of the importance of these tissues in SREBP-1c regulation. As describer previously, SREBP-1c is highly responsive to changes in nutritional status. Therefore, we performed experiments using fasting/refeeding regimes to study the impact of *Atgl* deletion in adipose tissue on SREBP-1c hepatic regulation in mice (30).

The analysis of SREBP-1c activation by WB showed that during fasting, P-SREBP-1c signals were very weak and no N-SREBP-1c signal was detected in AAKO and control groups (Figure 1B). These results are in agreement with the literature, which shows that SREBP-1c protein, as well as Srebf1 mRNA and other SREBP-1c target genes were significantly decreased in livers of fasted mice (19, 30, 73). After the mice were fed with a HCD, both the precursor and nuclear SREBP-1c signals gradually increased in both groups throughout the time course. However, we observed an upregulation of the active N-SREBP-1c isoform at the 6 h refed timepoint in the livers of AAKO mice compared to controls (Figure 1B and 1C).

Concomitantly, the hepatic expression of the SREBP-1c target genes *Fasn* and *Acaca* was significantly upregulated at 3 h and 6 h refed time points in AAKO mice, while *Srebf1* expression was increased also during fasting (Figure 1D).

In contrast to these findings, Schoiswohl et al., found in *ad libitum* fed AAKO mice that *Srebf1* mRNA expression was decreased in white adipose tissue (61). The expression of SREBP-2 target genes *Hmgcr* and *Hmgcs* was not affected in AAKO or control mice during fasting or refeeding (data not shown), suggesting a specific SREBP-1c response to ATGL deletion in the adipose tissue.

Different studies have demonstrated that AAKO mice display lower plasma NEFA levels (55, 60). In concordance with the literature, we confirmed significantly reduced plasma NEFA concentrations in AAKO mice during fasting because of the reduced release of FAs from adipose tissue due to the lack of ATGL (Figure 2A). In contrast, control mice with preserved lipolysis exhibited higher plasma NEFA levels compared to AAKO mice, reflecting the release of NEFAs from the adipose tissue during fasting.

Furthermore, during fasting, the NEFAs released from the adipose tissue by lipolysis are transported to the liver, where they are re-esterified for storage. Our results showed that the liver NEFA concentration was significantly reduced in the livers of AAKO mice during fasting compared to controls (Figure 2B). In line with these observations, the histological analysis of the liver showed dramatically decreased neutral lipid content in AAKO mice according to ORO staining (55, 60) and significantly reduced liver TG concentration determined by GC/FID (Figure 2D and 2E).

We confirmed previous studies, which demonstrate that ATGL-knockout animals show defective lipolysis and exhibit only half the fasting plasma NEFA concentration of controls (55). Altogether, these results are explained by the lack of plasma NEFAs transported to the liver from adipose tissue during lipolysis in AAKO mice.

Moreover, an important input from our study is that we described the plasma and liver NEFA composition in AAKO and control mice. This analysis demonstrated that the plasma unsaturated NEFA species were significantly reduced during fasting in AAKO mice compared to controls, whereas no changes were observed in saturated-NEFA species (Figure 2A). This finding was reflected in liver NEFA composition, which also showed lower uFA levels in AAKO mice (Figure 2B). These results support the evidence that ATGL preferentially hydrolyzes uFAs during lipolysis (55, 60), and this effect could account for the observed hepatic N-SREBP-1c upregulation in AAKO livers during refeeding.

These results supported our hypothesis that the lack of uFAs derived from adipose tissue during lipolysis can induce SREBP-1c upregulation in the liver of AAKO mice. Nonetheless, one fact that caught our attention was that while the main differences in plasma and liver NEFA were detected during fasting, the N-SREBP-1c protein and target genes were upregulated mainly at 6 h refeeding time point, when no significant differences in hepatic NEFA concentration or composition were detected anymore between AAKO and control mice.

These observations could sound contradictory. However, this can be explained because *in vitro* studies have shown that SREBP-1c requires an induction period to be cleavage-activated. In experiments where cells were treated with uFAs, SREBP-1c was suppressed only 4 hours after the addition of the treatment to the medium, reaching a higher inhibition 6 hours later, demonstrating that SREBP-1c activation does not respond immediately to exogenous FA levels (41). Therefore, the observed hepatic N-SREBP-1c induction in AAKO mice at the 6 h timepoint can be consequence of the lower plasma and liver uFA levels during fasting compared to control mice.

In addition, we observed an increased *Srebf1* expression in AAKO mice during fasting and the 3 h refed timepoint, when no N-SREBP-1c was detected by WB (Figure 1D).

These observations could be explained because a low amount of transcribed N-SREBP-1c may already be enough to induce the expression of these genes; however, the signal is below the WB detection threshold.

Since SREBP-1c is highly regulated by insulin in a process activated through the phosphorylation of AKT and the p70 S6 (S6) hepatic kinases (Ser 235/236 and Ser 240/244) (2, 19, 35, 36), we aimed to evaluate if the observed N-SREBP-1c upregulation in AAKO mice at 6 and 9 h refed time points was related to the improved insulin sensitivity that characterizes this genotype (61).

For this purpose, we analyzed the activation of the kinases involved in the insulin signaling pathway by WB using total liver extracts. The results showed significantly higher AKT and S6 phosphorylation in AAKO mice at 6 and 9 h refed time points compared to controls (Figure 3C and 3D). These results are in concordance with the literature, which describes a higher insulin sensitivity in AAKO mice (1, 61), evidenced by increased phosphorylation of PI3K and AKT in skeletal muscle *in vivo* (50). However, our results did not show differences in glucose and plasma insulin levels during refeeding (Figure 3A and 3B).

Therefore, we could not rule out the possibility that an insulin effect may partially induce SREBP-1c upregulation in AAKO mice, and to this point, it was unclear whether adipose-derived uFAs could directly suppress SREBP-1c activation in the liver or if the activation of the insulin signaling pathway was responsible for regulating SREBP-1c activation (74, 75).

In summary, our initial experiments using adipose ATGL-KO mice demonstrated that the FA synthesis by SREBP-1c is inhibited if uFAs derived from adipose tissue lipolysis are available, as observed in control mice. On the other hand, the absence of ATGL lipolysis in adipose tissue led to a significant upregulation of N-SREBP-1c, associated with lower plasma and liver uFA composition in AAKO mice.

However, since the liver is a key organ for lipid and FA synthesis, we aimed to further analyze the effect of specific *Atgl* deletion in the liver, where SREBP-1c is particularly active. Hence, we repeated the previously described fasting/refeeding experiment, but this time using specific liver ATGL-KO mice (ALKO) and control mice.

Similar to our findings in AAKO mice, we observed that the P-SREBP-1c WB signal was weak during fasting, whereas N-SREBP-1c was not detected in both ALKO and control groups, but the signal gradually increased after refeeding a HCD. Interestingly, a similar effect on N-SREBP-1c upregulation was observed in ALKO mice at the 6 h refed time point compared to controls (Figure 4B and 4C). The SREBP-1c target genes, *Fasn* and *Acaca*, were also significantly induced at this time point. In comparison, *Srebf1* expression showed an upregulation from fasting until 6 h after refeeding in ALKO mice compared to controls (Figure 4D).

Furthermore, ALKO mice showed similar levels of plasma NEFAs compared to controls (Figure 5A); this is explained by the fact that adipose tissue lipolysis was preserved and NEFAs were released to the plasma during fasting (48, 55). Comparable to our results, Wu et al., reported that ALKO mice showed no differences in plasma glucose and NEFA concentration compared to control mice after 6 h fasting (62). These results support that specific liver *Atgl* deletion confers a lower metabolic impact in mice, in contrast to the AAKO genotype.

Nonetheless, liver NEFA content was significantly higher in ALKO mice (Figure 5B). The presence of higher liver NEFA levels, despite the inhibition of ATGL-mediated hepatic lipolysis, could be explained by a reduced FA β-oxidation (62, 76), which in turn may increase liver NEFA levels (Figure 5B).

On the other hand, our findings showed a higher TG content in the liver during fasting, determined by GC/FID (Figure 5C) and ORO staining (Figure 5D), which is in agreement with the findings by Wu et al., who described marked hepatosteatosis and TG accumulation in fasted livers of ALKO mice compared to controls (62, 76). The higher TG content remained after refeeding but was significant only at 6 and 9 h time points (Figure 5C).

No differences were found in plasma glucose and insulin levels between ALKO and control mice (Figure 6A and 6B). Additionally, the WB analysis did not reveal changes in the insulin signaling pathway (Figure 6C and 6D), which indicates that the upregulated SREBP-1c cleavage-activation observed in ALKO mice is not related to insulin activation. These results indicate that *Atgl* liver deletion does not confer higher insulin sensitivity as observed in AAKO mice (61), suggesting that this effect is specifically related to ATGL activity in the adipose tissue.

However, it caught our attention that ALKO mice showed higher N-SREBP-1c activation in the liver (Figure 4B and 4C) despite normal plasma NEFA levels (Figure 5A), higher liver NEFA concentration (Figure 5B) and preserved ATGL lipolysis in the adipose tissue during fasting, in contrast to the observations in AAKO mice. Previous studies have shown that hepatic steatosis produces ER stress, which at the same time induces SREBP-1c overactivation, generating a vicious cycle (2) (29) (77). These findings could explain the higher SREBP-1c activation in ALKO mice at the 6h refed time point.

In summary, our data on ALKO mice showed that the absence of hepatic ATGL induces N-SREBP-1c activation in the liver after refeeding a HCD, compared to control mice (Figure 4B and 4C). However, the determination of plasma glucose and insulin levels plus the analysis of the insulin signaling pathway by WB, rule out the possibility that the observed N-SREBP-1c upregulation in this genotype was insulin-induced (78) (79) (80). These findings suggest N-SREBP-1c upregulation caused by ATGL inhibition in the liver, results from a mechanism independent of liver NEFAs and insulin regulation.

The liver is a key tissue for lipid and energetic homeostasis, where highly complex metabolic and biochemical reactions take place, producing hundreds of metabolites involved in a wide range of biochemical and molecular pathways, which could contribute to SREBP-1c regulation in ways that are not known yet. Therefore, further studies are needed in this field (29) (81).

As our findings in ALKO mice could not fully explain the significantly higher N-SREBP-1c induction compared to controls, we aimed to further analyze the hepatic SREBP-1c regulation, using a Flag-SREBP-1c cleavage-reporter system *in vitro,* containing the human Flag-SREBP-1c cassette, which allowed us to directly test the regulation of SREBP-1c cleavage-activation.

For this purpose, we tested the vector using the hepatic HepG2 cell line. The cells were transfected with the Flag-SREBP-1c vector and either treated under lipid-depleted conditions using lipoprotein depleted medium (LPDS) to induce SREBP-1c processing or treated with LPDS plus the addition of different FA to the medium (Figure 7A).

The results showed that the sFA 16:0 induced N-SREBP-1c cleavage similar to the lipid-depleted condition. Interestingly, treatment with uFA species strongly suppressed Flag-N-SREBP-1c cleavage activation similarly to 25-HC, a potent SREBP suppressor (Figure 7B and 7C). These results are in agreement with data published by Lee et al., who found that uFA treatment in CHO-7 cells inhibited SREBP-1c activation through INSIG-1 stabilization (6).

Our interesting results using the Flag-SREBF-1c cleavage-reporter vector *in vitro* prompted us to implement the same system *in vivo* to track SREBP-1c cleavage activation. Therefore, to be able to express the Flag-SREBF-1c expression cassette in mouse livers, we cloned it into an adenoviral vector under a CMV promoter using the AdEasy system, to allow its constitutive expression, resulting in the Ad-Flag-SREBP-1c cleavage-reporter vector (Figure 8A).

To test the system, we transduced wild-type mice with our construct. Four days later, mice were fasted overnight or fasted and refed a HCD overnight to evaluate their effect on SREBP-1c cleavage activation. Hepatic Flag-SREBP-1c was detected by WB using a Flag-specific antibody.

The results confirmed the constitutive expression of the Ad-Flag-SREBP-1c construct, as all mice exhibited a stable Flag-P-SREBP-1c signal, even under conditions where SREBP-1c transcription is very low, such as during fasting (Figure 8B and 8C). On the other hand, the HCD diet treatment strongly induced Flag-N-SREBP-1c cleavage activation and the expression of SREBP target genes (Figure 8D). As expected, feeding a HCD significantly increased glucose and insulin plasma levels (Figure 8E) and strongly induced insulin activation pathway, as shown in the WB (Figure 8F and 8G). Additionally, during fasting, wild type mice display higher plasma uNEFAs during fasting compared to mice fed a HCD, as shown in Figure 8H, which reflects the NEFAs released from adipose tissue lipolysis during fasting.

To analyze the effect of dietary FA composition on Ad-Flag-SREBP-1c cleavage activation, the experiment was repeated, but this time, the mice were fed an uFA-rich or sFA-rich diet for three consecutive days. Remarkably, when the mice were fed an uFA-rich diet, the Flag-N-SREBP-1c processing was significantly lower than in the sFA-rich diet group (Figure 9B and 9C). Subtle changes were found in *Fasn* expression, which was slightly upregulated in the sFA-rich diet group. Interestingly, these results emulated the observed *in vitro* SREBP-1c regulation by sFA or uFA in our HepG2 cell experiments, which is in line with the findings of Jing Xu et al 1999 (42) (Figure 7B and 7C).

The plasma glucose levels were unchanged between the groups (Figure 9E) and the insulin signaling pathway showed no differences between uFA and sFA diet (Figure 9F and 9G). These results account for a FA regulatory effect on SREBP-1c independent from an insulin effect on SREBP-1c transcription, at least using our Ad-Flag-SREBP-

1c cleavage reporter system. However higher levels of plasma insulin were recorded in the sFA diet group compared to uFA diet (Figure 9E).

The plasma NEFA analyses revealed a significant increase in 18:3 uFA concentration in the uFA-rich diet group. Conversely, in the sFA-rich diet group, the uFA concentration was significantly lower, while a significantly higher concentration of 16:0 sFA was recorded (Figure 9H). These findings reflect the dietary FA intake through supplementation with unsaturated flaxseed oil and saturated palm oil, respectively. These findings confirmed that our SREBP-1c cleavage activation reporter vector was sensitive to nutritional status and dietary FA acid composition.

On the other hand, at this point, we could not confirm whether the lack of lipolysis-derived uFAs caused the observed hepatic N-SREBP-1c upregulation or if it was induced by increased insulin sensitivity in AAKO mice (Figure 1B) (74, 82). Therefore, we aimed to focus our experiments on the fasting state, when the most significant differences in plasma and liver NEFAs were observed.

However, tracking SREBP-1c cleavage activation under starving conditions was challenging, because it is barely transcribed due to the lack of insulin. Nevertheless, since our Ad-Flag-SREBP-1c vector proved to be constitutively expressed regardless of insulin regulation, it would allow us to directly test if the FAs derived from adipose tissue lipolysis regulate SREBP-1c cleavage activation in the liver during fasting.

During fasting, a wide range of biochemical and metabolic reactions are induced, resulting in the activation of signaling molecules that can profoundly influence SREBP-1c activity. However, the study of SREBP-1c regulation during fasting is challenging due to its reduced transcription and its dependence on insulin regulation. To overcome this limitation, we created an adenoviral reporter vector that constitutively expresses Flag-SREBP-1c. This represents a helpful tool for studying SREBP-1c activation *in vivo,* avoiding the effects of factors that affect SREBP-1c transcription, such as insulin.

Therefore, to test our hypothesis, we transduced AAKO and control mice with the Ad-Flag-N-SREBP-1c cleavage reporter vector. Four days later, the mice were fasted overnight and then sacrificed. The hepatic Flag-P-SREBP-1c and Flag-N-SREBP-1c signals were assessed by WB.

AAKO and control mice livers showed similar levels of Flag-P-SREBP-1c expression during fasting (Figure 10B). However, to our surprise, AAKO mice livers showed a significant Flag-N-SREBP-1c cleavage activation compared to control mice during fasting, despite similar precursor levels (Figure 10C). In addition, *Fasn* expression was upregulated in AAKO group (Figure 10D). These results align with previous publications, demonstrating that dietary uFAs inhibit SREBP-1c cleavage-activation in the liver using a viral SREBP-1c reporter system (83).

Based on these observations, we hypothesized that the supply of external uFAs would inhibit N-SREBP-1c upregulation during fasting. Therefore, we repeated the same experiment, but this time, AAKO and Control mice were supplied intravenously with albumin-bound unsaturated oleic acid (18:1) at 6 and 9 h time points after the 12-hour fasting period.

The analysis of Liver NEFA composition measured by GC/FID showed lower 16:1 and 18:2 concentrations in AAKO mice compared to controls during fasting, which support the hypothesis that lower uFA liver availability induces SREBP-1c cleavage activation (Figure 10E).

Surprisingly, after we intravenously supplied oleic acid to the mice during fasting, the hepatic Flag-N-SREBP-1c cleavage activation was significantly reduced in AAKO mice, resulting in similar relative levels of proteolytically cleaved N-SREBP-1c levels compared to control mice (Figure 10B and 10C). Our results supported our hypothesis

that the reduced ATGL lipolysis-derived uFAs lead to N-SREBP-1c upregulation in the livers of AAKO mice during fasting.

Plasma glucose and insulin levels were significantly lower in AAKO mice during fasting, in concordance with the data reported by Kershaw et al. (61) (Figure 11A). Therefore, our results suggest a direct effect from lipolysis-derived uFAs on hepatic SREBP-1c regulation, which is not influenced by insulin during fasting (75).

The analysis of the insulin activation pathway in AAKO mice livers showed that AKT and Ser 235/236 were not active during fasting (Figure 11B). Therefore, we were only able to quantify S6 / Ser 240/44 activation, which was induced by oleic acid supplementation in both groups (Figure 11C). However, no significant differences in insulin regulation were found between AAKO and control groups (74). In contrast, previous studies suggest that uFAs, such as docosahexaenoic acid inhibit pAKT/ AKT activation *in vitro* (84).

On the other hand, it is well established that uFAs suppress SREBP-1c cleavage activation *in vitro* by modulating the transport of the SREBP-SCAP complex from the ER to the Golgi by INSIG stabilization (21) (85). To elucidate if uFAs regulate GFP-SCAP trafficking in the liver, we used a GFP-SCAP vector that was transfected into primary hepatocytes. Interestingly, treatment with different uFA species inhibited the SCAP-SREBP ER-to-Golgi transport in a similar manner as the strong SREBP-1c cleavage inhibitor, 25-HC. Treatment with sFAs showed no significant regulation. These results confirmed that uFAs act through the modulation of SREBP-1c trafficking in primary hepatocytes (Figure 12A and 12B).

Overall, our results demonstrated that uFAs inhibit SREBP-1c cleavage activation in the liver. However, several mechanisms could account for this inhibitory effect. As previously described, FAs derived from ATGL lipolysis act as energy substrates for other tissues during fasting. Additionally, these FAs work as signaling molecules

involved in diverse physiological and metabolic functions (46, 86). However, from the results of our study, we cannot conclude how these FAs act on other cellular levels and if they can regulate SREBP through additional mechanisms, which are discussed below.

It is known that uFAs inhibit SREBP-1c cleavage activation by stabilizing the proteins that regulate SREBP-1c trafficking in the cell. For example, INSIGs are the anchor proteins that retain the SCAP/SREBP complex in the ER membrane (31). The *Insig-1* and *Insig-2* genes are activated through different regulatory mechanisms. *Insig-1* expression is induced by feeding, while *Insig-2* increases upon fasting. It is possible that the uFAs released by ATGL lipolysis during fasting account for this effect, especially in the regulation of *Insig-2,* which is upregulated during fasting (43). However, deeper insight into this subject is needed.

In addition, previous reports have shown that uFAs modulate the SCAP transport to the Golgi apparatus via UBXD8, a protein associated with the ER degradation machinery. In a lipid-depleted cell environment, INSIG-1 is ubiquitinated by gp78 ligase, allowing it to bind to UBXD8, which recruits the valosin-containing proteins (VCP). This step enables the extraction of INSIG-1 from the ER membrane for subsequent degradation by proteasomes (44, 45, 85).

uFAs were shown to dissociate the UBXD8-VCP complex from INSIG-1, preventing its membrane dislocation and retaining the SREBP-SCAP complex in the ER membrane. As a consequence, the expression of SREBP-1c target genes was inhibited (6). This mechanism could account for the inhibitory effect of uFAs on SREBP-1c cleavage-activation observed in our *in vitro* and in vivo experiments.

Another aspect that could contribute to the inhibitory effect of uFAs on SREBP-1c activation is the Liver X Receptors (LXR), which induce FA and TG synthesis through SREBP-1c activation. Interestingly, uFAs were demonstrated to act as competitive inhibitors of LXR ligands and consequently suppress SREBP-1c cleavage activation (27) (32).

Moreover, Peroxisome Proliferator-Activated Receptors (PPARs) are a group of nuclear receptor proteins that play a key role in the regulation of genes required for fatty acid uptake and oxidation, TG hydrolysis and gluconeogenesis. Interestingly, fasting provides PPAR agonists that induce the expression of these receptors and ATGL-derived FAs function as ligands for PPAR-α, which drives mitochondrial fatty acid beta-oxidation (5). At the same time, PPAR-α drives *Insig-2a* transcription, and the translated INSIG2a protein suppresses SREBP-1c cleavage activation during fasting (43).

This mechanism could contribute to SREBP-1c mediated FA biosynthesis, which is suppressed when mice are fasted and induced when they are refed a HCD and low-fat diet (30). Therefore, *Insig-2a* is essential for the fasting / re-feeding mediated regulation of SREBP-1c in the liver. Additionally, ATGL genetic deletion in mice has an impact on PPAR-related pathways for FA and lipid synthesis, which should be further elucidated (5).

Another possible uFA-related mechanism is that the lipolysis-derived FAs are incorporated into the phospholipids of the ER membrane. It has been proposed that the membrane FA composition can modify SREBP-1c processing by inducing changes in the membrane fluidity and the disposition of other proteins, which can affect the trafficking of SREBP-1c/SCAP and INSIG complex from the ER to the Golgi apparatus (37) .

In conclusion, our findings demonstrate that ATGL-mediated lipolysis provides uFAs that can regulate hepatic SREBP-1c lipogenesis *in vivo*, revealing a previously unknown interplay between SREBP-1c and ATGL, the central regulators of lipogenesis and lipolysis (65). Nevertheless, we cannot rule out the possibility that ATGL lipolysis from other tissues contributes to this effect or that additional factors, such as insulin, contribute to SREBP-1c regulation during fasting. Therefore, additional studies are needed in this field.

Our insights take us one step further in understanding the molecular mechanisms that underlie the development of chronic and metabolic diseases related to lipid disorders.

SREBP-1c represents a promising target due to its critical importance for maintaining lipid and cellular homeostasis, which could expand the approaches for preventive and therapeutic strategies to mitigate the increasing incidence of these life-threatening diseases (12) (28).

5. REFERENCES

1. Schreiber R, Xie H, Schweiger M. Of mice and men: The physiological role of adipose triglyceride lipase (ATGL). Biochim Biophys Acta Mol Cell Biol Lipids. 2019;1864(6):880-99.
2. Eberle D, Hegarty B, Bossard P, Ferre P, Foufelle F. SREBP transcription factors: master regulators of lipid homeostasis. Biochimie. 2004;86(11):839-48.
3. Duan Y, Gong K, Xu S, Zhang F, Meng X, Han J. Regulation of cholesterol homeostasis in health and diseases: from mechanisms to targeted therapeutics. Signal Transduct Target Ther. 2022;7(1):265.
4. Horton JD, Goldstein JL, Brown MS. SREBPs: transcriptional mediators of lipid homeostasis. Cold Spring Harb Symp Quant Biol. 2002;67:491-8.
5. Haemmerle G, Moustafa T, Woelkart G, Buttner S, Schmidt A, van de Weijer T, et al. ATGL-mediated fat catabolism regulates cardiac mitochondrial function via PPAR-alpha and PGC-1. Nat Med. 2011;17(9):1076-85.
6. Lee JN, Zhang X, Feramisco JD, Gong Y, Ye J. Unsaturated fatty acids inhibit proteasomal degradation of Insig-1 at a postubiquitination step. J Biol Chem. 2008;283(48):33772-83.
7. Caturano A. Cardiovascular and Metabolic Disease: New Treatments and Future Directions 2.0. Biomedicines. 2024;12(6).
8. Zou P, Wang L. Dietary pattern and hepatic lipid metabolism. Liver Res. 2023;7(4):275-84.
9. Shimano H, Sato R. SREBP-regulated lipid metabolism: convergent physiology - divergent pathophysiology. Nat Rev Endocrinol. 2017;13(12):710-30.
10. Grabner GF, Xie H, Schweiger M, Zechner R. Lipolysis: cellular mechanisms for lipid mobilization from fat stores. Nat Metab. 2021;3(11):1445-65.
11. Yokoyama C, Wang X, Briggs MR, Admon A, Wu J, Hua X, et al. SREBP-1, a basic-helix-loop-helix-leucine zipper protein that controls transcription of the low density lipoprotein receptor gene. Cell. 1993;75(1):187-97.
12. Xiaoping Z, Fajun Y. Regulation of SREBP-Mediated Gene Expression. Sheng Wu Wu Li Hsueh Bao. 2012;28(4):287-94.
13. Hua X, Sakai J, Brown MS, Goldstein JL. Regulated cleavage of sterol regulatory element binding proteins requires sequences on both sides of the endoplasmic reticulum membrane. J Biol Chem. 1996;271(17):10379-84.
14. Rawson RB. The SREBP pathway--insights from Insigs and insects. Nat Rev Mol Cell Biol. 2003;4(8):631-40.
15. Brown MS, Goldstein JL. The SREBP pathway: regulation of cholesterol metabolism by proteolysis of a membrane-bound transcription factor. Cell. 1997;89(3):331-40.
16. Kim HJ, Miyazaki M, Man WC, Ntambi JM. Sterol regulatory element-binding proteins (SREBPs) as regulators of lipid metabolism: polyunsaturated fatty acids oppose cholesterol-mediated induction of SREBP-1 maturation. Ann N Y Acad Sci. 2002;967:34-42.
17. Goldstein JL, DeBose-Boyd RA, Brown MS. Protein sensors for membrane sterols. Cell. 2006;124(1):35-46.
18. Radhakrishnan A, Ikeda Y, Kwon HJ, Brown MS, Goldstein JL. Sterol-regulated transport of SREBPs from endoplasmic reticulum to Golgi: oxysterols block transport by binding to Insig. Proc Natl Acad Sci U S A. 2007;104(16):6511-8.
19. Daemen S, Kutmon M, Evelo CT. A pathway approach to investigate the function and regulation of SREBPs. Genes Nutr. 2013;8(3):289-300.

20. Sakai J, Duncan EA, Rawson RB, Hua X, Brown MS, Goldstein JL. Sterol-regulated release of SREBP-2 from cell membranes requires two sequential cleavages, one within a transmembrane segment. Cell. 1996;85(7):1037-46.
21. Matsuda M, Korn BS, Hammer RE, Moon YA, Komuro R, Horton JD, et al. SREBP cleavage-activating protein (SCAP) is required for increased lipid synthesis in liver induced by cholesterol deprivation and insulin elevation. Genes Dev. 2001;15(10):1206-16.
22. Ye J, DeBose-Boyd RA. Regulation of cholesterol and fatty acid synthesis. Cold Spring Harb Perspect Biol. 2011;3(7).
23. Caputo M, Zirpoli H, Torino G, Tecce MF. Selective regulation of UGT1A1 and SREBP-1c mRNA expression by docosahexaenoic, eicosapentaenoic, and arachidonic acids. J Cell Physiol. 2011;226(1):187-93.
24. Engelking LJ, Liang G, Hammer RE, Takaishi K, Kuriyama H, Evers BM, et al. Schoenheimer effect explained--feedback regulation of cholesterol synthesis in mice mediated by Insig proteins. J Clin Invest. 2005;115(9):2489-98.
25. Lee SH, Lee JH, Im SS. The cellular function of SCAP in metabolic signaling. Exp Mol Med. 2020;52(5):724-9.
26. Ou J, Tu H, Shan B, Luk A, DeBose-Boyd RA, Bashmakov Y, et al. Unsaturated fatty acids inhibit transcription of the sterol regulatory element-binding protein-1c (SREBP-1c) gene by antagonizing ligand-dependent activation of the LXR. Proc Natl Acad Sci U S A. 2001;98(11):6027-32.
27. Wang B, Tontonoz P. Liver X receptors in lipid signalling and membrane homeostasis. Nat Rev Endocrinol. 2018;14(8):452-63.
28. Horton JD, Goldstein JL, Brown MS. SREBPs: activators of the complete program of cholesterol and fatty acid synthesis in the liver. J Clin Invest. 2002;109(9):1125-31.
29. Kawano Y, Cohen DE. Mechanisms of hepatic triglyceride accumulation in non-alcoholic fatty liver disease. J Gastroenterol. 2013;48(4):434-41.
30. Horton JD, Bashmakov Y, Shimomura I, Shimano H. Regulation of sterol regulatory element binding proteins in livers of fasted and refed mice. Proc Natl Acad Sci U S A. 1998;95(11):5987-92.
31. Engelking LJ, Kuriyama H, Hammer RE, Horton JD, Brown MS, Goldstein JL, et al. Overexpression of Insig-1 in the livers of transgenic mice inhibits SREBP processing and reduces insulin-stimulated lipogenesis. J Clin Invest. 2004;113(8):1168-75.
32. Dixon ED, Nardo AD, Claudel T, Trauner M. The Role of Lipid Sensing Nuclear Receptors (PPARs and LXR) and Metabolic Lipases in Obesity, Diabetes and NAFLD. Genes (Basel). 2021;12(5).
33. Sato R. Sterol metabolism and SREBP activation. Arch Biochem Biophys. 2010;501(2):177-81.
34. Han Y, Hu Z, Cui A, Liu Z, Ma F, Xue Y, et al. Post-translational regulation of lipogenesis via AMPK-dependent phosphorylation of insulin-induced gene. Nat Commun. 2019;10(1):623.
35. Krycer JR, Sharpe LJ, Luu W, Brown AJ. The Akt-SREBP nexus: cell signaling meets lipid metabolism. Trends Endocrinol Metab. 2010;21(5):268-76.
36. Li S, Ogawa W, Emi A, Hayashi K, Senga Y, Nomura K, et al. Role of S6K1 in regulation of SREBP1c expression in the liver. Biochem Biophys Res Commun. 2011;412(2):197-202.
37. Rong X, Wang B, Palladino EN, de Aguiar Vallim TQ, Ford DA, Tontonoz P. ER phospholipid composition modulates lipogenesis during feeding and in obesity. J Clin Invest. 2017;127(10):3640-51.
38. Beceiro S, Pap A, Czimmerer Z, Sallam T, Guillen JA, Gallardo G, et al. Liver X Receptor Nuclear Receptors Are Transcriptional Regulators of Dendritic Cell Chemotaxis. Mol Cell Biol. 2018;38(10).
39. Chen G, Liang G, Ou J, Goldstein JL, Brown MS. Central role for liver X receptor in insulin-mediated activation of Srebp-1c transcription and stimulation of fatty acid synthesis in liver. Proc Natl Acad Sci U S A. 2004;101(31):11245-50.

40. Yoshikawa T, Shimano H, Yahagi N, Ide T, Amemiya-Kudo M, Matsuzaka T, et al. Polyunsaturated fatty acids suppress sterol regulatory element-binding protein 1c promoter activity by inhibition of liver X receptor (LXR) binding to LXR response elements. J Biol Chem. 2002;277(3):1705-11.
41. Hannah VC, Ou J, Luong A, Goldstein JL, Brown MS. Unsaturated fatty acids down-regulate srebp isoforms 1a and 1c by two mechanisms in HEK-293 cells. J Biol Chem. 2001;276(6):4365-72.
42. Xu J, Nakamura MT, Cho HP, Clarke SD. Sterol regulatory element binding protein-1 expression is suppressed by dietary polyunsaturated fatty acids. A mechanism for the coordinate suppression of lipogenic genes by polyunsaturated fats. J Biol Chem. 1999;274(33):23577-83.
43. Lee JH, Kang HS, Park HY, Moon YA, Kang YN, Oh BC, et al. PPARalpha-dependent Insig2a overexpression inhibits SREBP-1c processing during fasting. Sci Rep. 2017;7(1):9958.
44. Lee JN, Kim H, Yao H, Chen Y, Weng K, Ye J. Identification of Ubxd8 protein as a sensor for unsaturated fatty acids and regulator of triglyceride synthesis. Proc Natl Acad Sci U S A. 2010;107(50):21424-9.
45. Lee JN, Song B, DeBose-Boyd RA, Ye J. Sterol-regulated degradation of Insig-1 mediated by the membrane-bound ubiquitin ligase gp78. J Biol Chem. 2006;281(51):39308-15.
46. Alves-Bezerra M, Cohen DE. Triglyceride Metabolism in the Liver. Compr Physiol. 2017;8(1):1-8.
47. Lass A, Zimmermann R, Oberer M, Zechner R. Lipolysis - a highly regulated multi-enzyme complex mediates the catabolism of cellular fat stores. Prog Lipid Res. 2011;50(1):14-27.
48. Zechner R. FAT FLUX: enzymes, regulators, and pathophysiology of intracellular lipolysis. EMBO Mol Med. 2015;7(4):359-62.
49. Zechner R, Kienesberger PC, Haemmerle G, Zimmermann R, Lass A. Adipose triglyceride lipase and the lipolytic catabolism of cellular fat stores. J Lipid Res. 2009;50(1):3-21.
50. Trites MJ, Clugston RD. The role of adipose triglyceride lipase in lipid and glucose homeostasis: lessons from transgenic mice. Lipids Health Dis. 2019;18(1):204.
51. Olzmann JA, Richter CM, Kopito RR. Spatial regulation of UBXD8 and p97/VCP controls ATGL-mediated lipid droplet turnover. Proc Natl Acad Sci U S A. 2013;110(4):1345-50.
52. Zimmermann R, Strauss JG, Haemmerle G, Schoiswohl G, Birner-Gruenberger R, Riederer M, et al. Fat mobilization in adipose tissue is promoted by adipose triglyceride lipase. Science. 2004;306(5700):1383-6.
53. Grabner GF, Zimmermann R, Schicho R, Taschler U. Monoglyceride lipase as a drug target: At the crossroads of arachidonic acid metabolism and endocannabinoid signaling. Pharmacol Ther. 2017;175:35-46.
54. Zimmermann R, Lass A, Haemmerle G, Zechner R. Fate of fat: the role of adipose triglyceride lipase in lipolysis. Biochim Biophys Acta. 2009;1791(6):494-500.
55. Eichmann TO, Kumari M, Haas JT, Farese RV, Jr., Zimmermann R, Lass A, et al. Studies on the substrate and stereo/regioselectivity of adipose triglyceride lipase, hormone-sensitive lipase, and diacylglycerol-O-acyltransferases. J Biol Chem. 2012;287(49):41446-57.
56. Harayama T, Shimizu T. Roles of polyunsaturated fatty acids, from mediators to membranes. J Lipid Res. 2020;61(8):1150-60.
57. Lass A, Zimmermann R, Haemmerle G, Riederer M, Schoiswohl G, Schweiger M, et al. Adipose triglyceride lipase-mediated lipolysis of cellular fat stores is activated by CGI-58 and defective in Chanarin-Dorfman Syndrome. Cell Metab. 2006;3(5):309-19.
58. Ding L, Huwyler F, Long F, Yang W, Binz J, Wernle K, et al. Glucose controls lipolysis through Golgi PtdIns4P-mediated regulation of ATGL. Nat Cell Biol. 2024;26(4):552-66.
59. Kintscher U, Foryst-Ludwig A, Haemmerle G, Zechner R. The Role of Adipose Triglyceride Lipase and Cytosolic Lipolysis in Cardiac Function and Heart Failure. Cell Rep Med. 2020;1(1):100001.

60. Haemmerle G, Lass A, Zimmermann R, Gorkiewicz G, Meyer C, Rozman J, et al. Defective lipolysis and altered energy metabolism in mice lacking adipose triglyceride lipase. Science. 2006;312(5774):734-7.
61. Schoiswohl G, Stefanovic-Racic M, Menke MN, Wills RC, Surlow BA, Basantani MK, et al. Impact of Reduced ATGL-Mediated Adipocyte Lipolysis on Obesity-Associated Insulin Resistance and Inflammation in Male Mice. Endocrinology. 2015;156(10):3610-24.
62. Wu JW, Wang SP, Alvarez F, Casavant S, Gauthier N, Abed L, et al. Deficiency of liver adipose triglyceride lipase in mice causes progressive hepatic steatosis. Hepatology. 2011;54(1):122-32.
63. Fougerat A, Schoiswohl G, Polizzi A, Regnier M, Wagner C, Smati S, et al. ATGL-dependent white adipose tissue lipolysis controls hepatocyte PPARalpha activity. Cell Rep. 2022;39(10):110910.
64. Schreiber R, Hofer P, Taschler U, Voshol PJ, Rechberger GN, Kotzbeck P, et al. Hypophagia and metabolic adaptations in mice with defective ATGL-mediated lipolysis cause resistance to HFD-induced obesity. Proc Natl Acad Sci U S A. 2015;112(45):13850-5.
65. Pena de la Sancha P, Wieser BI, Schauer S, Reicher H, Sattler W, Breinbauer R, et al. Lipolysis-derived fatty acids are needed for homeostatic control of sterol element-binding protein-1c driven hepatic lipogenesis. Commun Biol. 2025;8(1):588.
66. Engelking LJ, Kuriyama H, Hammer RE, Horton JD, Brown MS, Goldstein JL, et al. Overexpression of Insig-1 in the livers of transgenic mice inhibits SREBP processing and reduces insulin-stimulated lipogenesis. Journal of Clinical Investigation. 2004;113(8):1168-75.
67. Folch J, Lees M, Sloane Stanley GH. A simple method for the isolation and purification of total lipides from animal tissues. The Journal of biological chemistry. 1957;226(1):497-509.
68. D'Orazio P, Burnett RW, Fogh-Andersen N, Jacobs E, Kuwa K, Kulpmann WR, et al. Approved IFCC recommendation on reporting results for blood glucose: International Federation of Clinical Chemistry and Laboratory Medicine Scientific Division, Working Group on Selective Electrodes and Point-of-Care Testing (IFCC-SD-WG-SEPOCT). Clin Chem Lab Med. 2006;44(12):1486-90.
69. Schmittgen TD, Livak KJ. Analyzing real-time PCR data by the comparative C(T) method. Nat Protoc. 2008;3(6):1101-8.
70. Schneider CA, Rasband WS, Eliceiri KW. NIH Image to ImageJ: 25 years of image analysis. Nat Methods. 2012;9(7):671-5.
71. Shao W, Machamer CE, Espenshade PJ. Fatostatin blocks ER exit of SCAP but inhibits cell growth in a SCAP-independent manner. J Lipid Res. 2016;57(8):1564-73.
72. Schweiger M, Romauch M, Schreiber R, Grabner GF, Hutter S, Kotzbeck P, et al. Pharmacological inhibition of adipose triglyceride lipase corrects high-fat diet-induced insulin resistance and hepatosteatosis in mice. Nat Commun. 2017;8:14859.
73. Shimano H, Yahagi N, Amemiya-Kudo M, Hasty AH, Osuga J, Tamura Y, et al. Sterol regulatory element-binding protein-1 as a key transcription factor for nutritional induction of lipogenic enzyme genes. J Biol Chem. 1999;274(50):35832-9.
74. Matsuzaka T, Shimano H. Insulin-dependent and -independent regulation of sterol regulatory element-binding protein-1c. J Diabetes Invest. 2013;4(5):411-2.
75. Owen JL, Zhang Y, Bae SH, Farooqi MS, Liang G, Hammer RE, et al. Insulin stimulation of SREBP-1c processing in transgenic rat hepatocytes requires p70 S6-kinase. Proc Natl Acad Sci U S A. 2012;109(40):16184-9.
76. Ong KT, Mashek MT, Bu SY, Greenberg AS, Mashek DG. Adipose triglyceride lipase is a major hepatic lipase that regulates triacylglycerol turnover and fatty acid signaling and partitioning. Hepatology. 2011;53(1):116-26.

77. Kim JY, Garcia-Carbonell R, Yamachika S, Zhao P, Dhar D, Loomba R, et al. ER Stress Drives Lipogenesis and Steatohepatitis via Caspase-2 Activation of S1P. Cell. 2018;175(1):133-45 e15.
78. Li T, Guo W, Zhou Z. Adipose Triglyceride Lipase in Hepatic Physiology and Pathophysiology. Biomolecules. 2021;12(1).
79. Fuchs CD, Radun R, Dixon ED, Mlitz V, Timelthaler G, Halilbasic E, et al. Hepatocyte-specific deletion of adipose triglyceride lipase (adipose triglyceride lipase/patatin-like phospholipase domain containing 2) ameliorates dietary induced steatohepatitis in mice. Hepatology. 2022;75(1):125-39.
80. Ong KT, Mashek MT, Bu SY, Mashek DG. Hepatic ATGL knockdown uncouples glucose intolerance from liver TAG accumulation. FASEB J. 2013;27(1):313-21.
81. Smati S, Regnier M, Fougeray T, Polizzi A, Fougerat A, Lasserre F, et al. Regulation of hepatokine gene expression in response to fasting and feeding: Influence of PPAR-alpha and insulin-dependent signalling in hepatocytes. Diabetes Metab. 2020;46(2):129-36.
82. Kienesberger PC, Lee D, Pulinilkunnil T, Brenner DS, Cai L, Magnes C, et al. Adipose triglyceride lipase deficiency causes tissue-specific changes in insulin signaling. J Biol Chem. 2009;284(44):30218-29.
83. Takeuchi Y, Yahagi N, Izumida Y, Nishi M, Kubota M, Teraoka Y, et al. Polyunsaturated fatty acids selectively suppress sterol regulatory element-binding protein-1 through proteolytic processing and autoloop regulatory circuit. J Biol Chem. 2010;285(15):11681-91.
84. Huang LH, Chung HY, Su HM. Docosahexaenoic acid reduces sterol regulatory element binding protein-1 and fatty acid synthase expression and inhibits cell proliferation by inhibiting pAkt signaling in a human breast cancer MCF-7 cell line. BMC Cancer. 2017;17(1):890.
85. Yang T, Espenshade PJ, Wright ME, Yabe D, Gong Y, Aebersold R, et al. Crucial step in cholesterol homeostasis: sterols promote binding of SCAP to INSIG-1, a membrane protein that facilitates retention of SREBPs in ER. Cell. 2002;110(4):489-500.
86. Nguyen P, Leray V, Diez M, Serisier S, Le Bloc'h J, Siliart B, et al. Liver lipid metabolism. J Anim Physiol Anim Nutr (Berl). 2008;92(3):272-83.

6. APPENDIX

Supplementary Table 1. qPCR Primer sequences.

Primer Pair	Forward	Reverse
m*Fasn*	GGCCCCTCTGTTAATTGGCT	GGATCTCAGGGTTGGGGTTG
m*Acaca*	GGCCAGTGCTATGCTGAGAT	CCAGGTCGTTTGACATAATGG
m*18s*	GTAACCCGTTGAACCCCATT	CCATCCAATCGGTAGTAGCG
mSrebf1	GGAGCCATGGATTGCACATT	GGCCCGGGAAGTCACTGT
mEnd_Srebf1	CTGACAGGTGAAATCGGCG	AATCCATGGCTCCGTGGTC

Supplementary Table 2. Antibodies

Antibodies				
Reagent type	**Designation**	**Source or reference**	**Identifiers**	**Additional information**
Antibody	Anti-SREBP-1c, clone 2A4. (Mouse monoclonal)	Abcam	ab3259	(1:500)
Antibody	Anti-SREBP-1c clone 20B12. (Rabbit monoclonal)	Merck	MABS1987	(1:500)
Antibody	Anti-FLAG® M2 (Mouse monoclonal)	Sigma-Aldrich	F3165	(1:500)
Antibody	Anti-FLAG® M2-Peroxidase (HRP) (Mouse monoclonal)	Sigma-Aldrich	A8592	(1:500)
Antibody	Anti-GFP- avictoria antibody. (Rabbit polyclonal)	Abcam	ab290	(1:500)
Antibody	Anti-GM130, clone 35. (Mouse monoclonal)	BD Biosiences	610822	(1:250)
Antibody	Anti-Rabbit IgG (H+L), Alexa Fluor 488 coupled. (Goat polyclonal)	Invitrogen	A11034	(1:250)
Antibody	Anti-Mouse IgG (H+L), Alexa Fluor 594 coupled. (Mouse polyclonal)	Invitrogen	A11005	(1:250)
Antibody	Anti-mouse Immunoglobulins/HRP. (Goat polyclonal)	Dako	P0477	(1:3000)
Antibody	Anti-rabbit Immunoglobulins/HRP (Pig polyclonal)	Dako	P0217	(1:3000)